System and Propagation Availability Analysis for NASA's Advanced Air Transportation Technologies

Dr. Okechukwu C. Ugweje
Department of Electrical and Computer Engineering
The University of Akron
Akron, OH 44325-3904

Final Report for:
Research Grant No. NAG3-2279

Sponsored by:

Space Communications Division
NASA Glenn Research Center, Cleveland, OH 44135

July 2000

ABSTRACT

This report summarizes the research on the System and Propagation Availability Analysis for NASA's project on Advanced Air Transportation Technologies (AATT). The objectives of the project were to determine the communication systems requirements and architecture, and to investigate the effect of propagation on the transmission of space information. In this report, results from the first year investigation are presented and limitations are highlighted.

To study the propagation links, an understanding of the total system architecture is necessary since the links form the major component of the overall architecture. This study was conducted by way of analysis, modeling and simulation on the system communication links. The overall goals was to develop an understanding of the space communication requirements relevant to the AATT project, and then analyze the links taking into consideration system availability under adverse atmospheric weather conditions.

This project began with a preliminary study of the end-to-end system architecture by modeling a representative communication system in MATLAB SIMULINK. Based on the defining concepts, the possibility of computer modeling was determined. The investigations continue with the parametric studies of the communication system architecture. These studies were also carried out with SIMULINK modeling and simulation. After a series of modifications, two end-to-end communication links were identified as the most probable models for the communication architecture. Link budget calculations were then performed in MATHCAD and MATLAB for the identified communication scenarios.

A remarkable outcome of this project is the development of a graphic user interface (GUI) program for the computation of the link budget parameters in real time. Using this program, one can interactively compute the link budget requirements after supplying a few necessary parameters. It provides a framework for the eventual automation of several computations required in many experimental NASA missions.

For the first year of this project, most of the stated objectives were accomplished. We were able to identify probable communication systems architectures, model and analyze several communication links, perform numerous simulation on different system models, and then develop a program for the link budget analysis.

However, most of the work is still unfinished. The effect of propagation on the transmission of information in the identified communication channels has not been performed. Propagation effects cannot be studied until the system under consideration is identified and characterized. To study the propagation links, an understanding of the total communications architecture is necessary. It is important to mention that the original project was intended for two years and the results presented here are only for the first year of research. It is prudent therefore that these efforts be continued in order to obtain a complete picture of the system and propagation availability requirements.

INTRODUCTION

The National Aeronautics and Space Administration (NASA) has been in the forefront of technological innovation. One of such recent innovations is the Advanced Air Transportation Technologies (AATT) initiative. This project initiated by NASA in 1995 [1], is concerned with the development of a robust air transportation system involving the integration of space and ground communication infrastructure such as the Ground Stations, Aircrafts, Ships, Satellites, Radio Towers, and Airport Control Center. The AATT project is responsible for the definition, research and development of such high-risk communication technology, as an integral part of the new global Air Traffic Management (ATM) system [1]. AATT project was to identify the necessary components, define and analyze the design requirements, and outline the necessary specifications for the implementation of the ATM. This is a very revolutionary concept that has tremendous potential for both commercial and military applications. However, before this concept can be implemented, the ideas expressed in the concept definition [1] must be researched, designed, tested and integrated into a cohesive and robust communication system.

The importance of communication subsystem in the AATT project cannot be overemphasized, since the radio frequency (RF) and space communication infrastructure forms one of the major parts of the project. Successful implementation depends heavily on robust nature of the communication subsystem. It has been noted in [1] that future air traffic management will require a very robust communication environment allowing a seamless information exchange between users and service providers, thereby supporting the collaboration and decision making process required to achieve free flight objectives. The infrastructure will be capable of supporting ground-to-air communications, satellite-to-airplane communications, satellite-to-ground communications, and perhaps satellite-to-satellite communications. In addition, these communication scenarios take place at different modes, ranges, locations, frequencies, data rates and other operational requirements. Hence, efficient communication systems are crucial to realizing the AATT concepts.

To this end, the understanding of the communication links and the different communication scenarios that could arise is immensely important. That was the focus of the first year research - to define and analyze the communication link scenarios. Results from these investigations are described in this report, and limitations are identified whenever applicable.

Statement of the Problem

Current aeronautic communication systems are still based on old technology developed in the 1920's. The communication systems are characterized by:

1. The use of AM radio link between pilots and ground station.

2. The use of S-mode for data communications which is of little used due to high costs.

3. The use of VHF ground based links operating at 25 kHz per channel in congested frequency band and in high density traffic areas.

4. The requirement for 50,000 ground radio towers to cover continental USA (CONUS) with no current capability for VHF Data Link.

5. The use of High Frequency (HF) communications primarily for oceanic over-the-horizon communication with low reliability and low quality of communication.

6. The use of link-by-link communication each with individual link requirements. This means that the type of communication link in use depends on the phase of flight

7. The limited use of satellite communications except for the oceanic communications through INMARSAT. This satellite link has low data rate capability and not inexpensive

Rationale for Research

With emerging communication technologies (e.g. satellite, smart antennas, Ka-band, etc.), the above mentioned limitations in traditional avionics communication can be significantly improved. Instead of communicating on a link-by-link basis, integrated communication systems providing total systems response could be developed. This will lead to significant increase in system performance such as increased reliability, increased capacity, increased availability, increased security and improved safety condition.

Goals of Research

In this research, we studied the system requirements and communication architecture to meet ATM needs. The study develops a system level modeling and simulation capability by simulating and modeling the individual communications links and providing an unbiased analysis of those channels. It included performance analysis of the communication links and a suggestion on overall system integration. This study will enhance the integration of system communication architecture.

APPROACH

In this research, we followed a systematic top-down approach in our analysis. The study begins with a preliminary study or review of the system design requirements from the original concept definitions. The focus was on the system communication architecture. From the preliminary study, several tasks were outlined and then each of the outlined tasks was performed systematically. The main purpose of the preliminary study was to determine the feasibility of modeling a complete communication system using MATLAB SIMULINK. This project was performed by a group of engineers from NASA Glenn Research Center (GRC), Project Development and Integration Branch, led by Dr. Roberto Acosta and another group from The University of Akron led by the Principal Investigator (PI).

The preliminary study was followed by parametric study of realistic communication systems architecture. The parametric studies were performed in MATHCAD and MATLAB SIMULINK. Simulation was performed for coded and uncoded communication system models, thereby assessing the effectiveness of the coding gain, since coding is one of the proven ways of mitigating fade effects [2]. In addition, the channel models included the assessment of multiple access capabilities of the links. Three types of multiple access techniques were investigated namely: Time Division Multiple Access (TDMA), Frequency Division Multiple Access (FDMA), and Code Division Multiple Access (CDMA).

All simulations of the communication systems in this project were performed with MATLAB SIMULINK [3]. SIMULINK is an interactive, block-diagram-based tool for modeling and analyzing dynamic systems. It is tightly coupled with MATLAB and supported by numerous Blocksets and Toolboxes. It is commonly available and is widely used in the Industry and the Universities all over the country. More especially, it is not very difficult to learn compared to similar software packages. Hence, the choice of MATLAB for this project is justified.

Next, the identification and characterization of all possible links scenarios were conducted. Because of the practical implementation issues, similar links structures were grouped together, thereby reducing the overall communication scenarios to two primary links. The identified communication scenarios were modeled, analyzed and simulated. The analysis involves MATHCAD and MATLAB modeling and simulation, and the computation of link budget parameters. Because of the importance of link budget in space communications, attempts ware made to automate the computation. This led to the development of an interactive graphic user interface (GUI) program used for link budget calculations. This program provides an efficient way of obtaining and evaluating link budget parameters instantaneously. Although this program is developed for AATT, efforts are underway to modify it for a more generalized link budget analysis.

In the next section, step-by-step implementation of this project is presented. In order to present a cohesive picture, each model description is followed by the results whenever applicable.

TECHNICAL ANALYSIS

A. Preliminary Study

The purpose of the preliminary study was to develop an understanding of the concept definitions and the systems implementation requirements. To this effect, representative communication systems were modeled in software and verified that results closely match theoretical values. This serves as a benchmark for validating the results obtained from software modeling and simulation.

We began by modeling an uncoded and a Gray-coded communication system. A simple two-channel model is shown in Fig. 1. The first channel is uncoded and the second channel is Gray-coded. This figure is used to compute the performance as a function of energy per bit or energy per symbol. The implementation uses generic building blocks and parameters contained in MATLAB SIMULINK, Communications Blocksets and the DSP Blocksets.

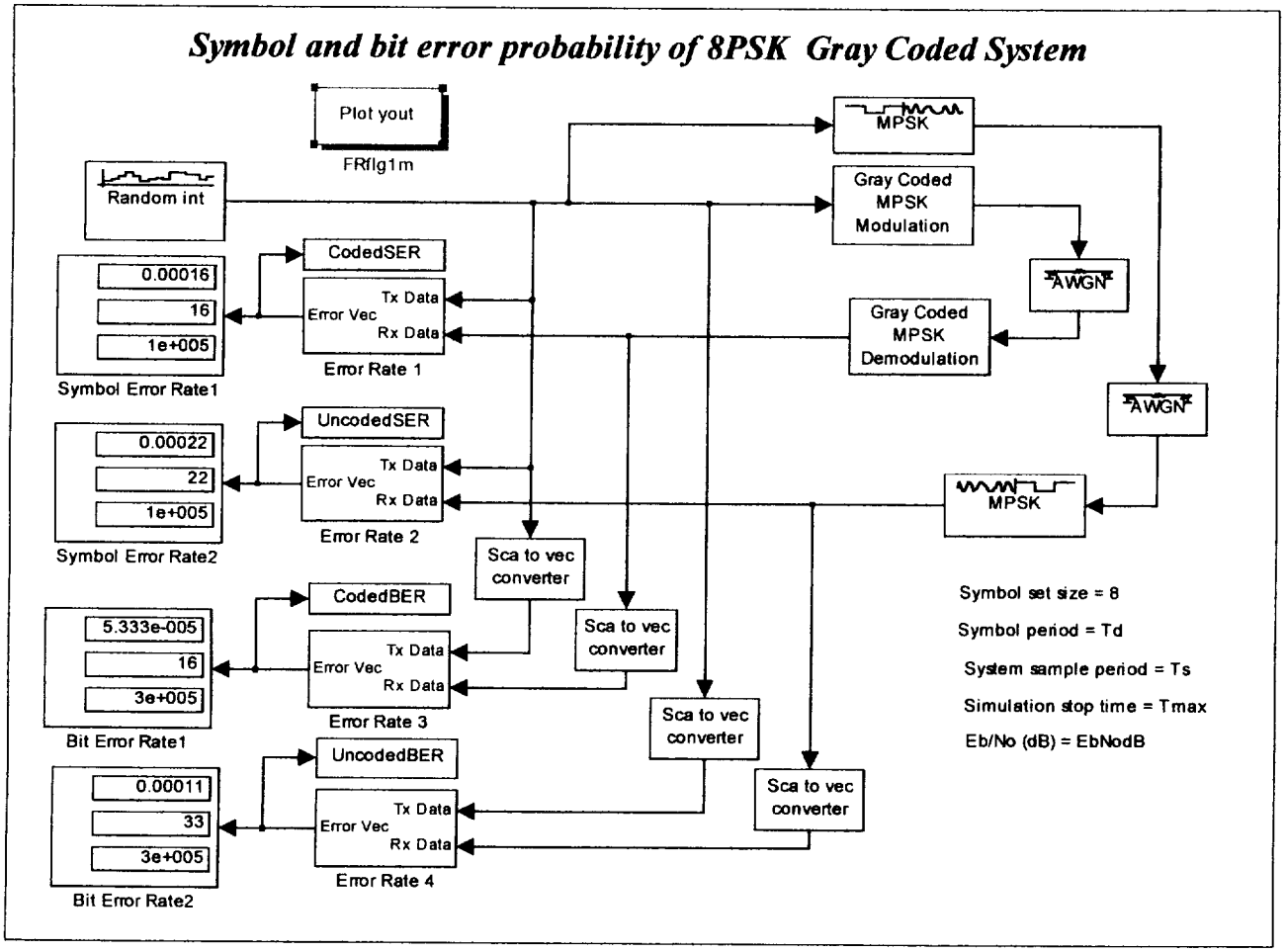

Fig. 1: Model of Uncoded and Gray-Coded Communication System with 8PSK Modulation

In this figure, each block represents a subsystem containing elementary building blocks. This figure was used to validate SIMULINK as an appropriate software modeling tool. It was also used to investigate the coding gain. In this model, a random integer generator is used as the signal source. One branch of the signal is simply modulated and then passed through an additive white Gaussian noise (AWGN) channel, while the other half is Gray-coded, 8PSK modulated and then passed through a similar channel. The transmitted signal is compared to the received signal after demodulation and decoding. The error of the detection is calculated and displayed in real time using the error rate calculator and display block. Also, note that this model is used to compute both symbol and bit error rate by simply converting symbol to bits using the scalar-to-vector converter block.

This simulation is controlled by a MATLAB mfile program named ***Graycode8PSKm.m*** embedded and masked with the SIMULINK model. This program is used to control the simulation time, iteration, tolerance and many other simulation settings. This method was found to be very efficient because to change a simulation parameter requires only editing the program. This program also controls the plotting algorithm. Please note that this is the technique adopted throughout the modeling in this project and requires no further explanation.

The result of this simulation is given in Fig. 2 for 8PSK modulation, where the BER performance is plotted as a function of the E_b/N_0. Both the theoretical performance and the simulated performance are shown. Theoretical bounds (upper and lower bounds) were also plotted.

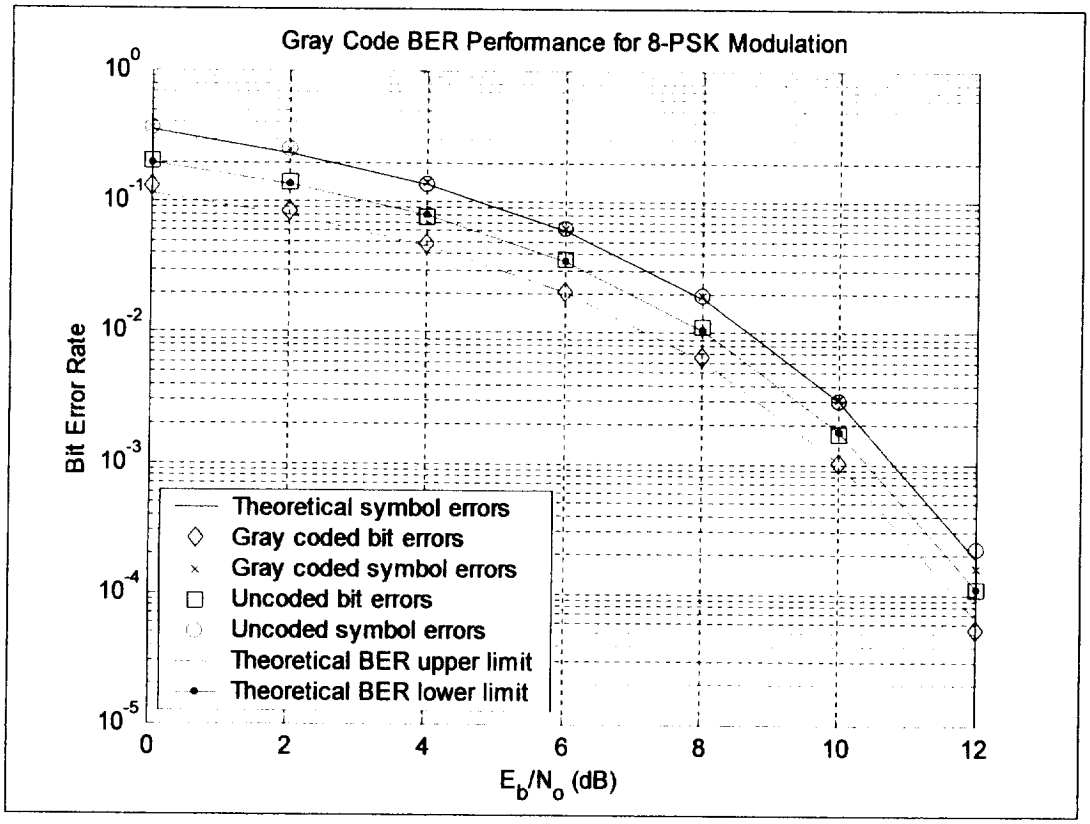

Fig. 2: BER Performance of Uncoded and Gray-Coded System with 8PSK Modulation.

In the above figure, the correspondence between theoretical, uncoded and Gray-coded symbol error rate is observed. Similar correspondence is also evident between theoretical BER lower bound and uncoded BER, whereas the theoretical BER upper bound corresponds with Gray-coded BER. In the figure, solid lines are used to denote theoretical values and symbols denote simulated values. The improvement in performance as E_b/N_0 increases is clearly shown

Figure 1 can easily be modified for a generalized M-ary (M > 2) simulation with similar results shown in Fig. 3. An obvious result of Fig. 3 is that as the number of symbols increases, system performance also decreases, which is consistent with the expected result.

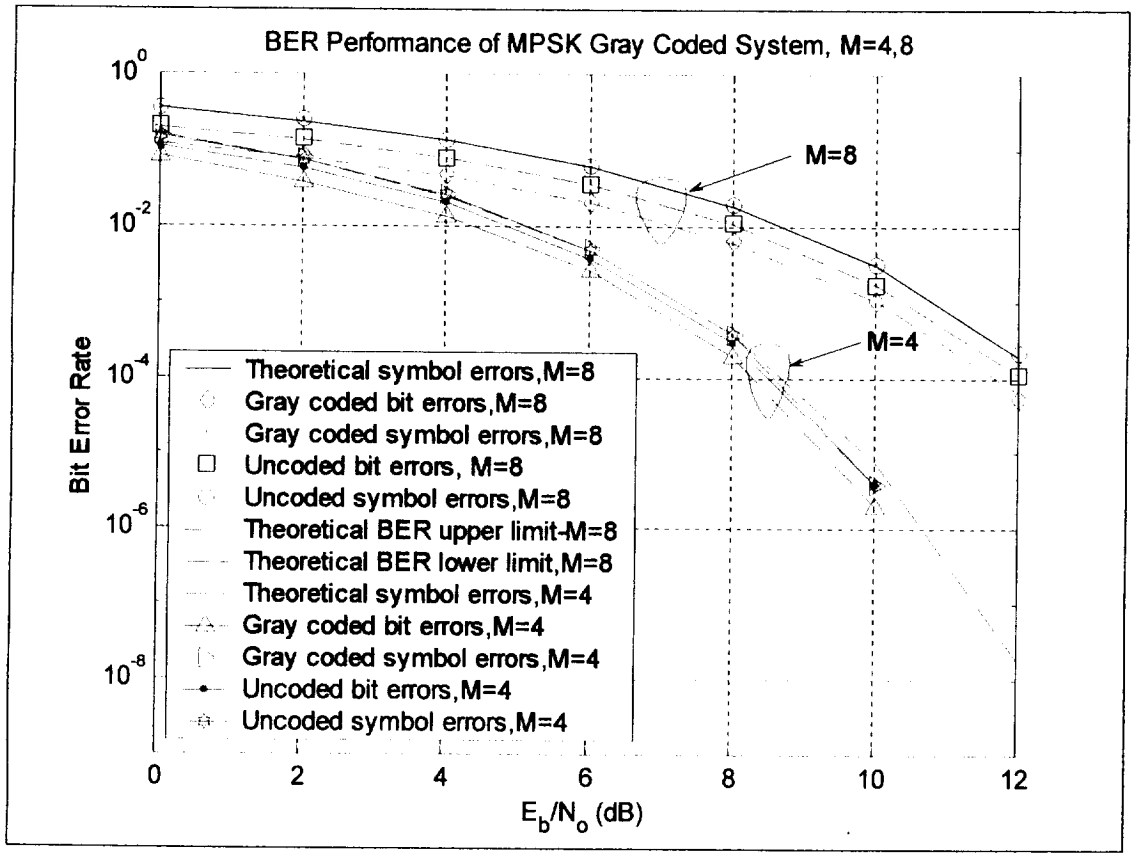

Fig. 3: BER Performance of Uncoded and Gray-Coded System for $M = 4$ & $M = 8$.

In Fig. 4, a two channel BPSK system model is shown illustrating the ability of multiplexing different users in a common communication channel. Two sources, signal_1 and signal_2, represent two users communicating through two separate but identical channels. The result of this simulation is similar to the results shown in Figs. 2 and 3.

One of the outcomes of this preliminary study is the validation of MATLAB modeling and simulation of end-to-end communication system. Since the results in Figs. 2 and 3 are identical to theoretical values, one can conclude that SIMULINK modeling of communication systems is valid. Hence, subsequent analysis was divided into different task processes spanning from

parametric studies to link evaluation. Next, each of the tasks is analyzed in details using practical system parameters and considering practical communication systems requirements.

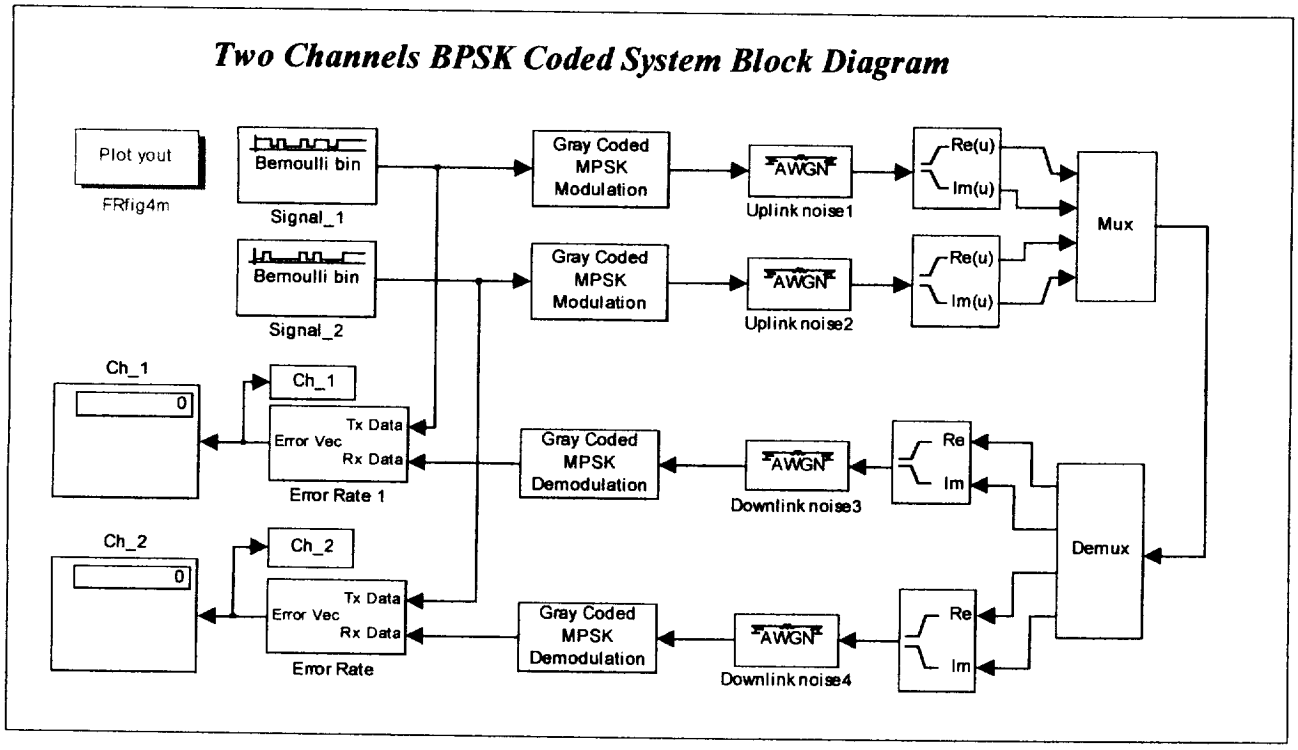

Fig. 4: Two-channel BPSK Communication System Model

B. Parametric Study of the Communications System Architecture

As in the preliminary study, the parametric study also involves the simulation of communication systems using SIMULINK. The difference is the consideration of more practical system parameters and consideration of AATT system requirements. In the simulation, communication systems with and without coding were considered. The models were more realistic with practical coding techniques. Two types of coding techniques were investigated namely Convolutional Coding and Reed-Solomon Coding. These two coding techniques are commonly used in wireless and satellite communication systems. For both the coded and uncoded models, the selected modulation scheme used throughout this project is the binary phase shift keying (BPSK).

1. Convolutional Coded Communication System

In this task, the objective was to investigate system performance under different convolutional coding rates and constraint lengths. Both punctured and unpunctured convolutional coding techniques were considered. The coding rates and the corresponding constraint lengths used in this simulation are given in Table 1.

Figure 5 illustrates the model of single channel unpunctured convolutional coded communication system. Notice that the coded signal is decoded with a Viterbi decoder and that buffering is used after encoding and before decoding. The result is shown in Fig. 6. As expected, the result indicates better performance as E_b/N_0 increases. It was observed that high E_b/N_0 requires more simulation iteration and hence takes more time obtain a valid result

Table 1: Convolutional Coding Parameters

Convolutional Coding Techniques				
Punctured			Unpunctured	
Original Rate	New Rate	Constraint Length	Rate	Constraint Length
1/2	2/3	7	1/2	5
1/2	3/4	7	1/2	7
1/2	7/8	7	-	-

The performance of coded and uncoded system was also investigated using the general model in Fig. 5. The result shown in Fig. 7 compares convolutional coded system with uncoded system. It is obvious from the plot that when coding is applied system performance is much better for E_b/N_0 greater than 1.5 dB. This plot also shows that the use of coding is ineffective at very low E_b/N_0.

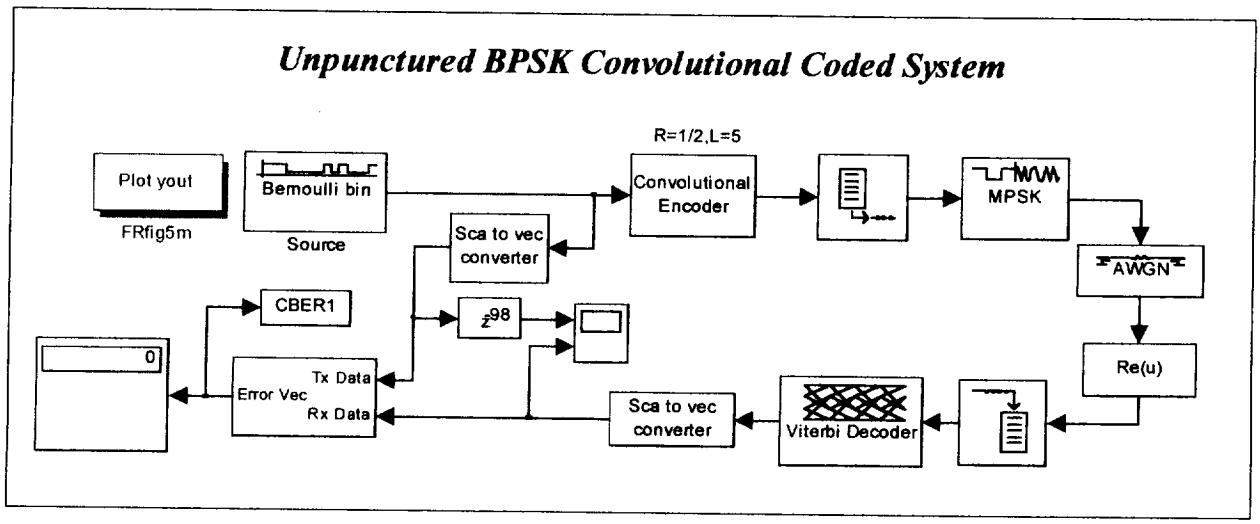

Fig. 5: Single Channel Convolutional Coding @ Rate 1/2, Constraint Length 5.

Figure 8 illustrates a two channel communication system showing the ability to multiplex convolutional coded channels. The configuration is similar to Fig. 5 except that two uplink and two downlink channels are used and multiplexing is applied. The reason is to differentiate users that may have different channel requirements. For example, an airplane-to-airplane communications may have different uplink or downlink requirements from airplane-

to-gateway communications. So, the different channels can be modified to account for individual channel requirements.

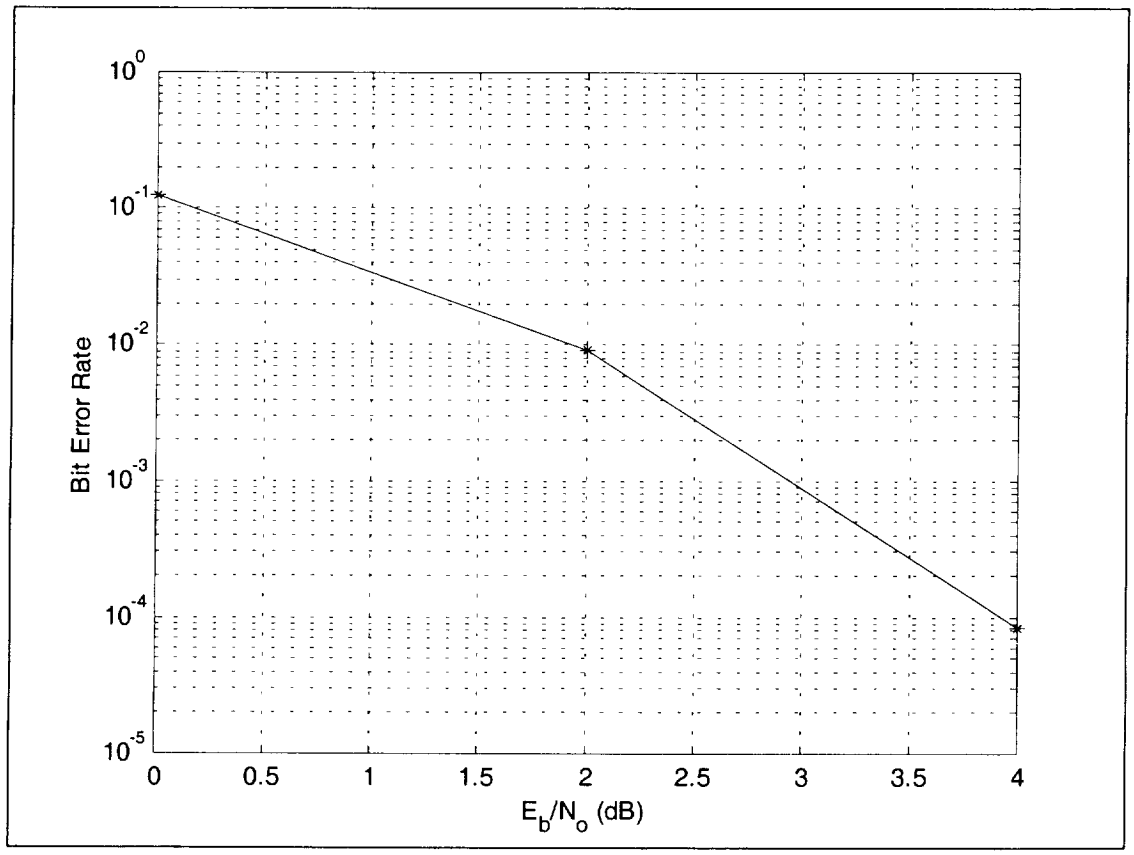

Fig. 6: BER Performance of Unpunctured Convolutional Coded System.

In this model, one channel is perturbed by adjusting the noise variance of the AWGN channel in comparison to the other channel. The adjustment of the variance can be used to indicate different noise factor or fade events in one channel compared to the other. The effect of the disparity in noise variance accounts for the shift in performance as E_b/N_o increases. At lower E_b/N_o, both systems have similar performance, which is reasonable, especially at high E_b/N_0.

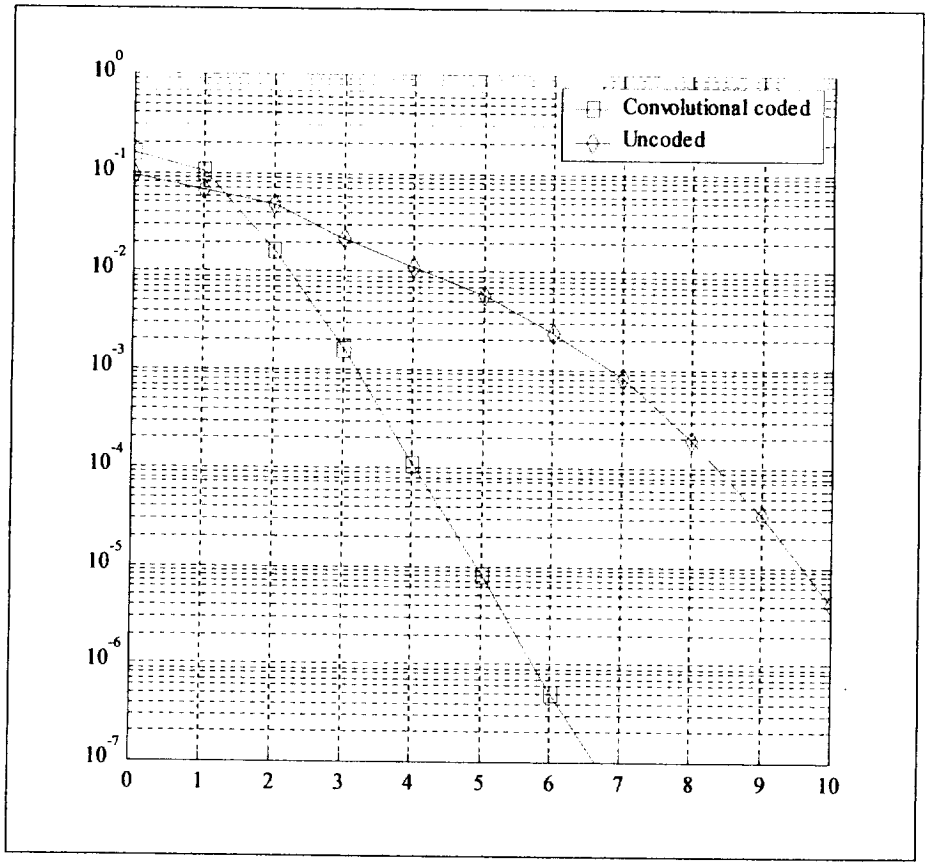

Fig. 7: BER Performance of Coded and Uncoded Communication System Model.

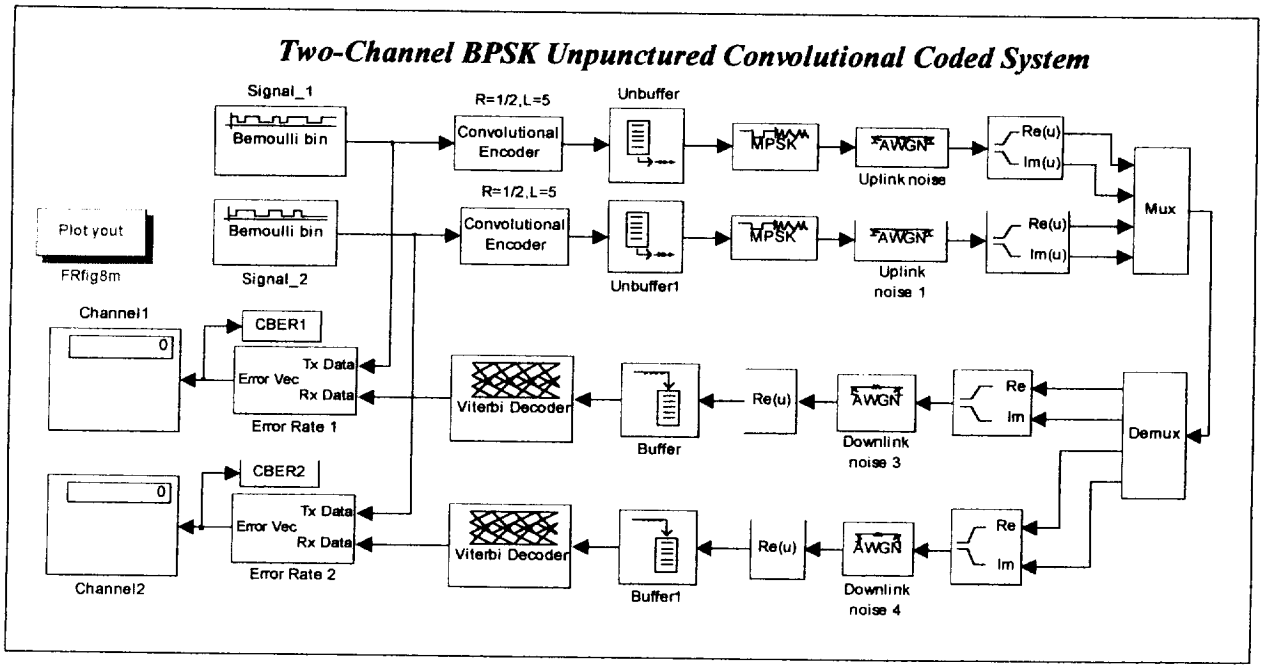

Fig. 8: Two-Channel Unpunctured Convolutional Coded System, Rate ½, Constraint Length 5.

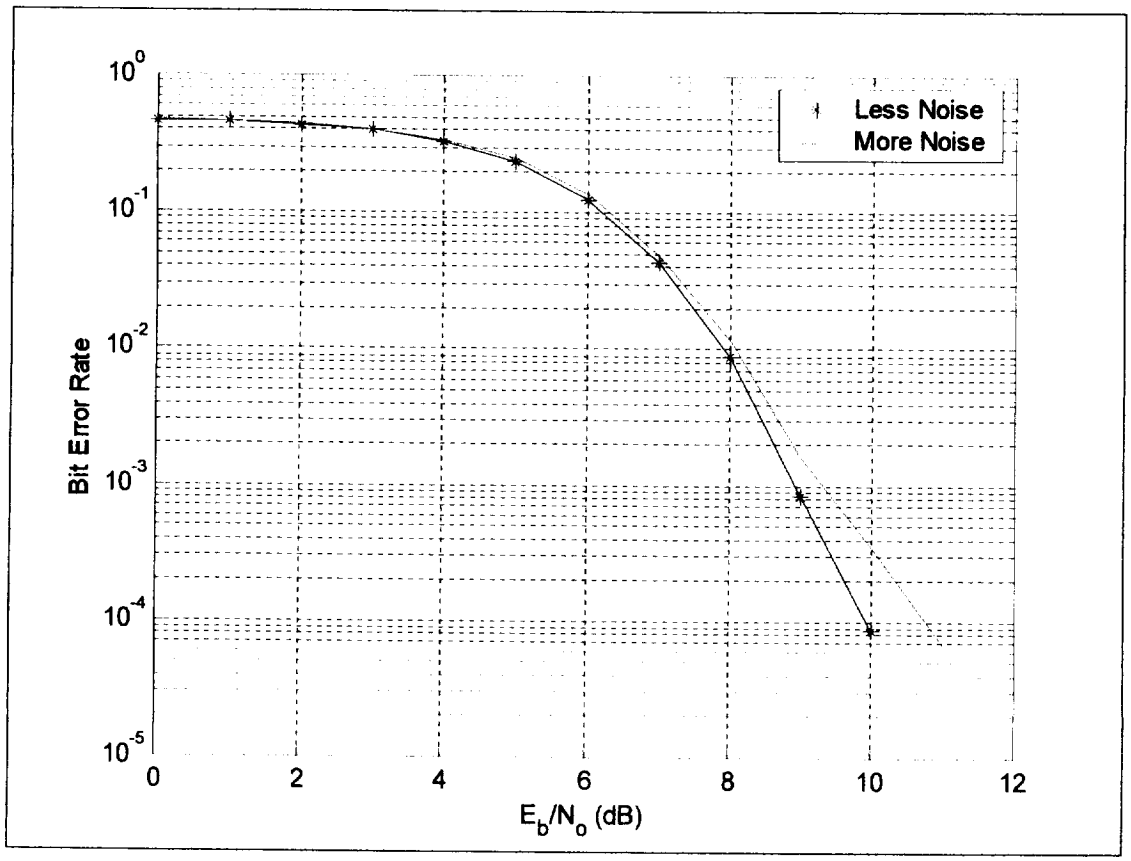

Fig. 9: BER Performance of Two-Channel Unpunctured Convolutional Coded System.

Figures 10 through 15 are concerned with the simulation of punctured convolutional coded communication systems. A punctured convolutional code is a high-rate code obtained by the periodic elimination (puncturing) of specific code symbols from the output of a low-rate encoder [4]. This type of coding is useful for high data rates transmission systems. It is also useful for systems prone to high error probability performance. Since the defining concept of AATT suggest the application of high data rate with small error, investigating such error coding technique is most appropriate [5]. In particular, we studied the effect of a rate change from low rate to three high rate convolutional codes. The high rate codes were obtained from the same rate 1/2 convolutional code.

Figure 10 shows the basic structure of single channel punctured convolutional coded system. After encoding, puncturing is applied before the signal is modulated. The effect of puncturing is reversed at the receiver by erasure insertion, before Viterbi decoding. As indicated in Table 1 Constraint Length 7 is used for all punctured convolutional coded system in this project.

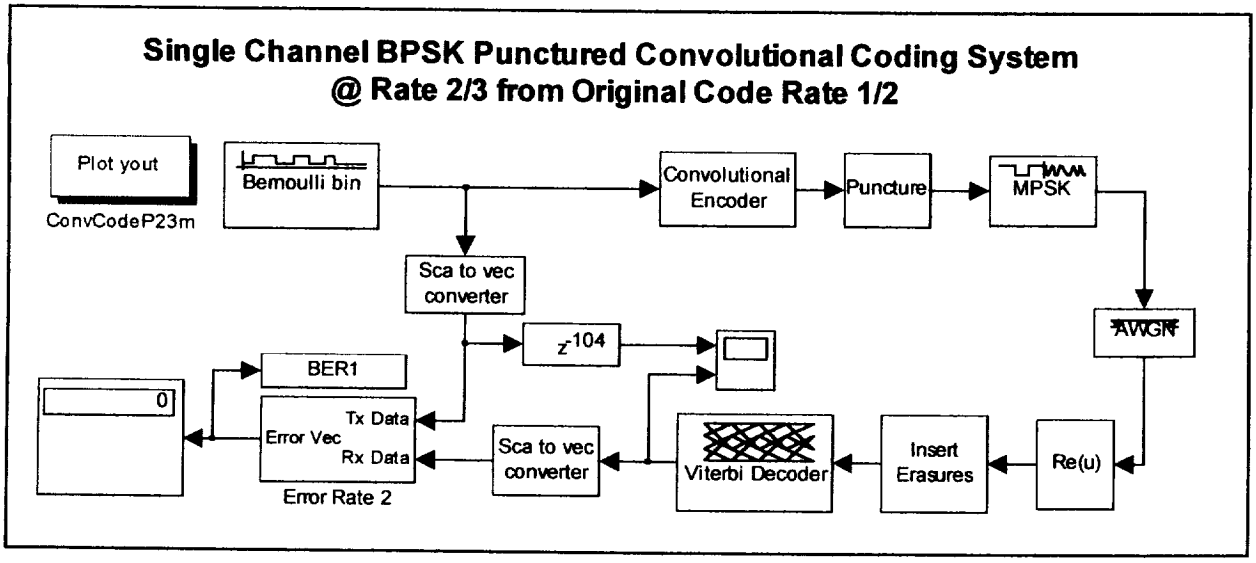

Fig. 10: Single Channel Punctured Convolutional Coded System Model @ Rate 2/3.

Using the model in Fig. 10, other high rate codes such as rate 3/4 and rate 7/8 convolutional codes were simulated individually. The rate is modified from the original 1/2 rate by modifying the puncturing and erasure algorithm [4], [5]. The results for rate 2/3, rate 3/4, and rate 7/8 punctured convolutional coded systems are shown in Figs. 11, 12, and 13, respectively.

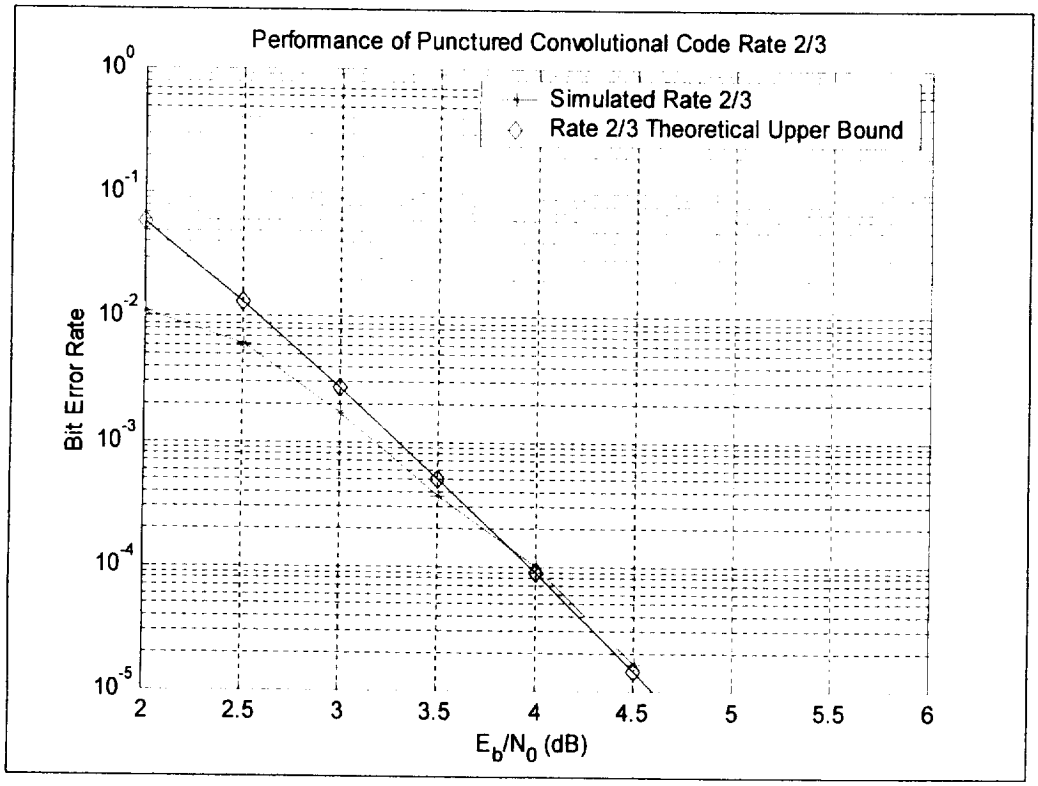

Fig. 11: BER Performance of Punctured Convolutional Coded System @ Rate 2/3.

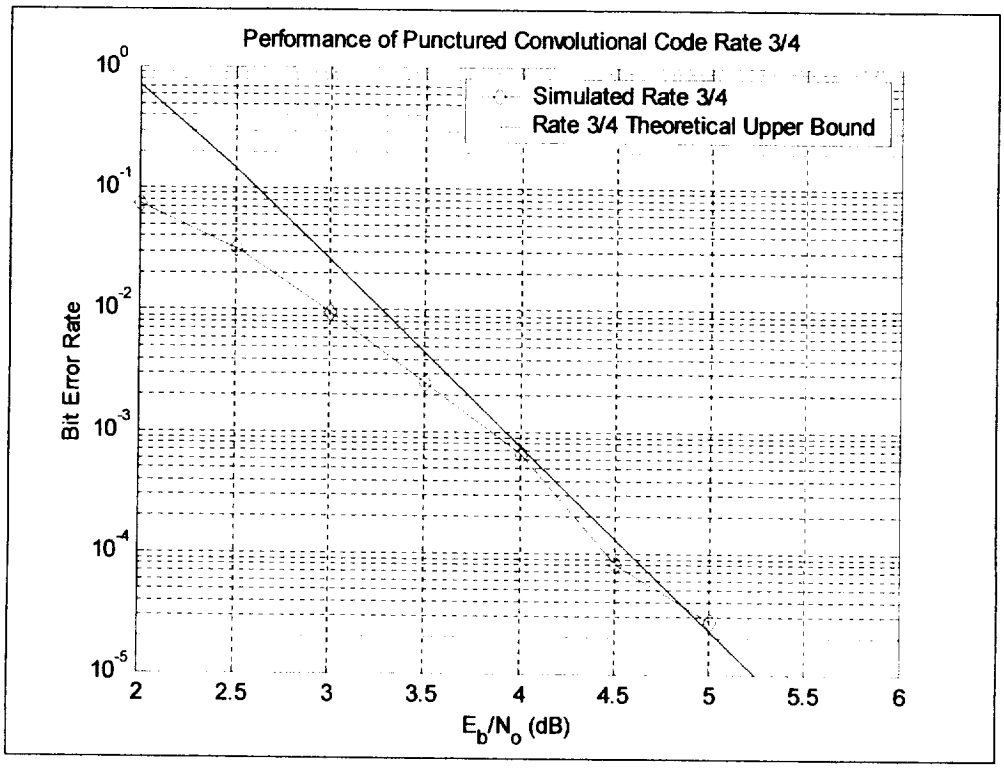

Fig. 12: BER Performance of Punctured Convolutional Coded System @ Rate 3/4.

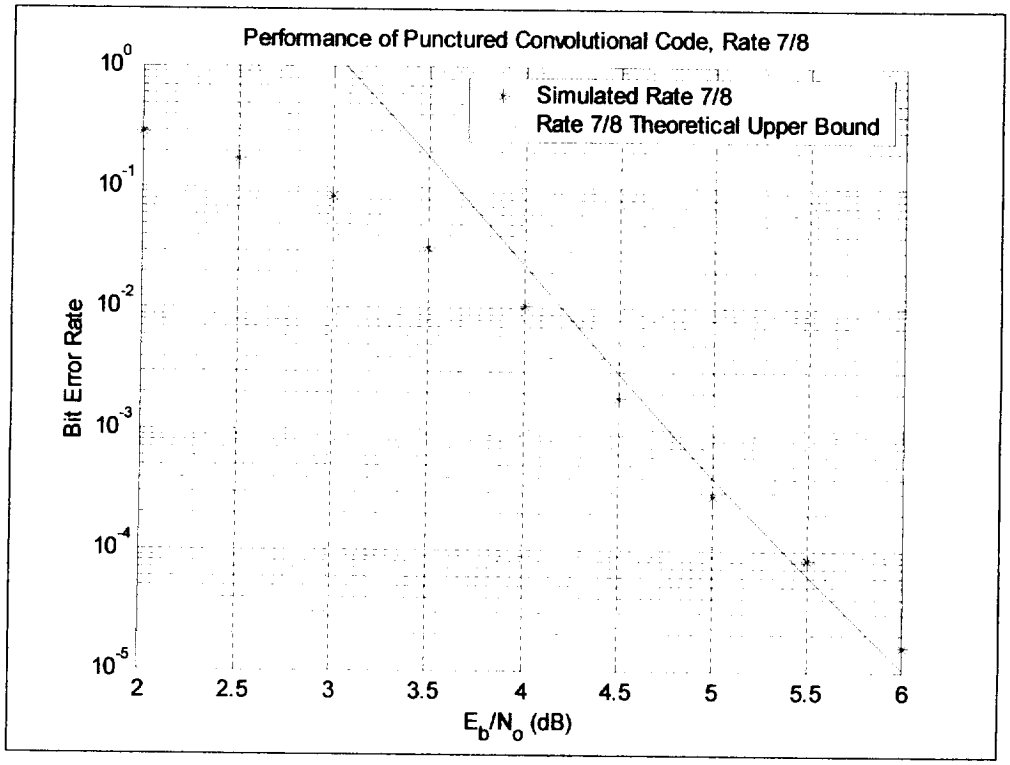

Fig. 13: BER Performance of Punctured Convolutional Coded System @ Rate 7/8.

For the three figures, the solid lines indicate the theoretical upper bound [4], [5], [6], while the star and diamond points indicate the actual simulated value. For each case, notice the close match for high E_b/N_0 and the larger deviation for low E_b/N_0.

One can also combine the three high-rate punctured codes in one simulation block diagram as shown in Fig. 14. The three high-rate convolutional codes are combined into one model and simulated at the same time. All the channels are made identical since we are only investigating the effect of puncturing (rate change) on system performance. The corresponding result for this model is shown in Fig. 15. This is equivalent to combining Figs. 11, 12 and 13.

The effect of constraint length on system performance was also studied. This is shown in Fig. 16. The two commonly used constraint lengths are Constraint Length 5 and 7. For example, convolutional coding of Rate 1/2 Constraint Length 5 is used in ACTS implementation [7].

The model shown in Fig. 16 is for unpunctured convolutional coded system. The structure of this model is the same as in Fig. 5 except that we have combined the two constraint lengths. The result of this simulation is shown in Fig. 17. The figure indicates that performance is degraded with increasing constraint length.

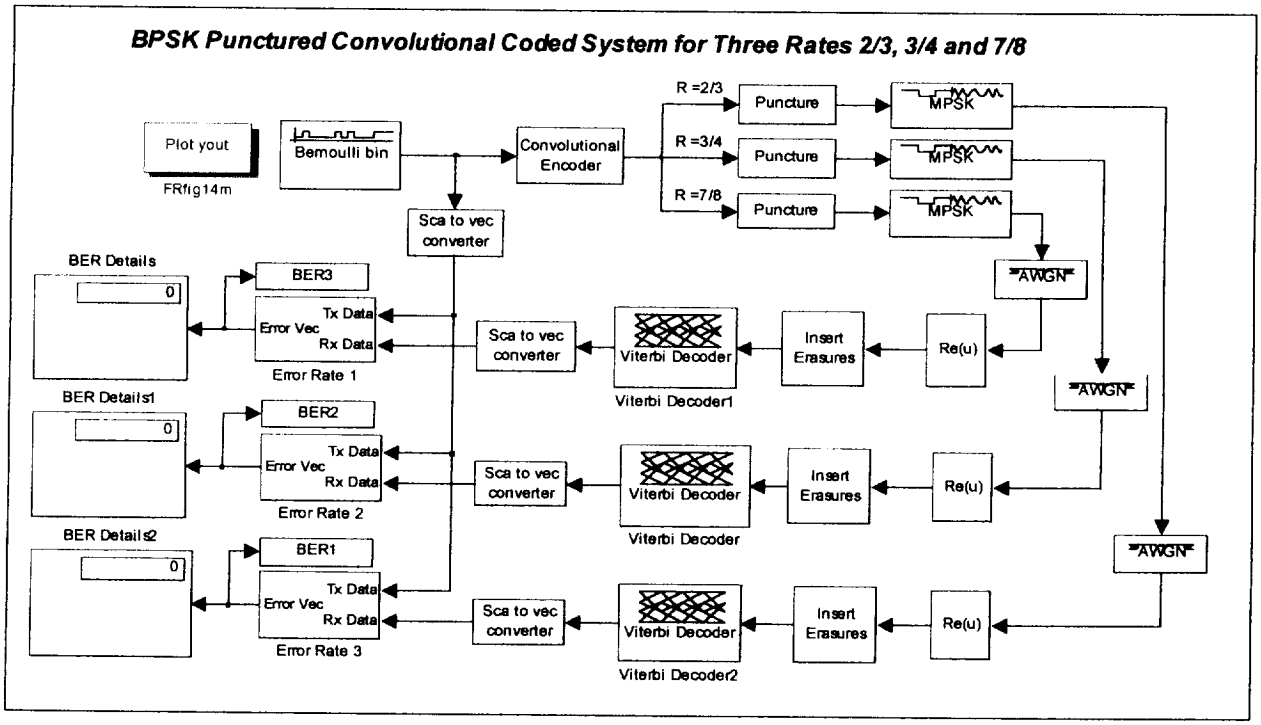

Fig. 14: Variable Rate Punctured Convolutional Coded Communication System.

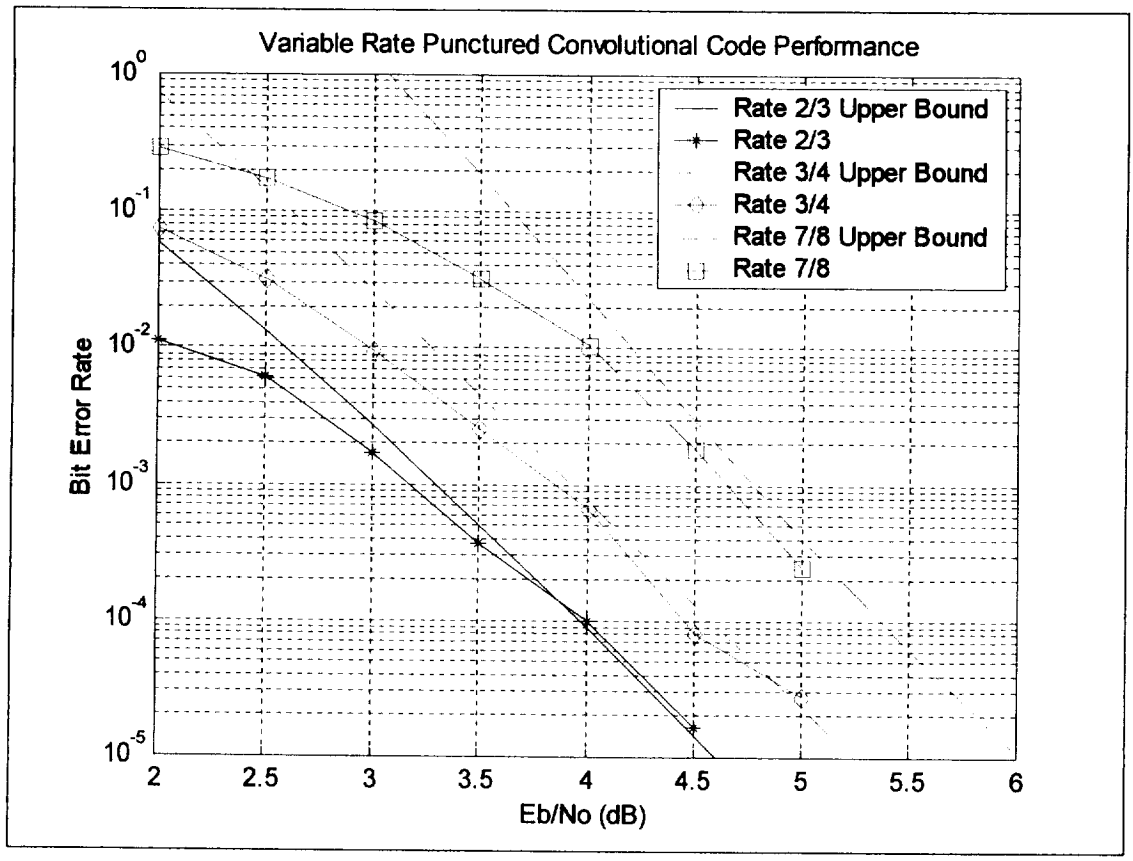

Fig. 15: Results of Variable Rate Convolutional Coded System

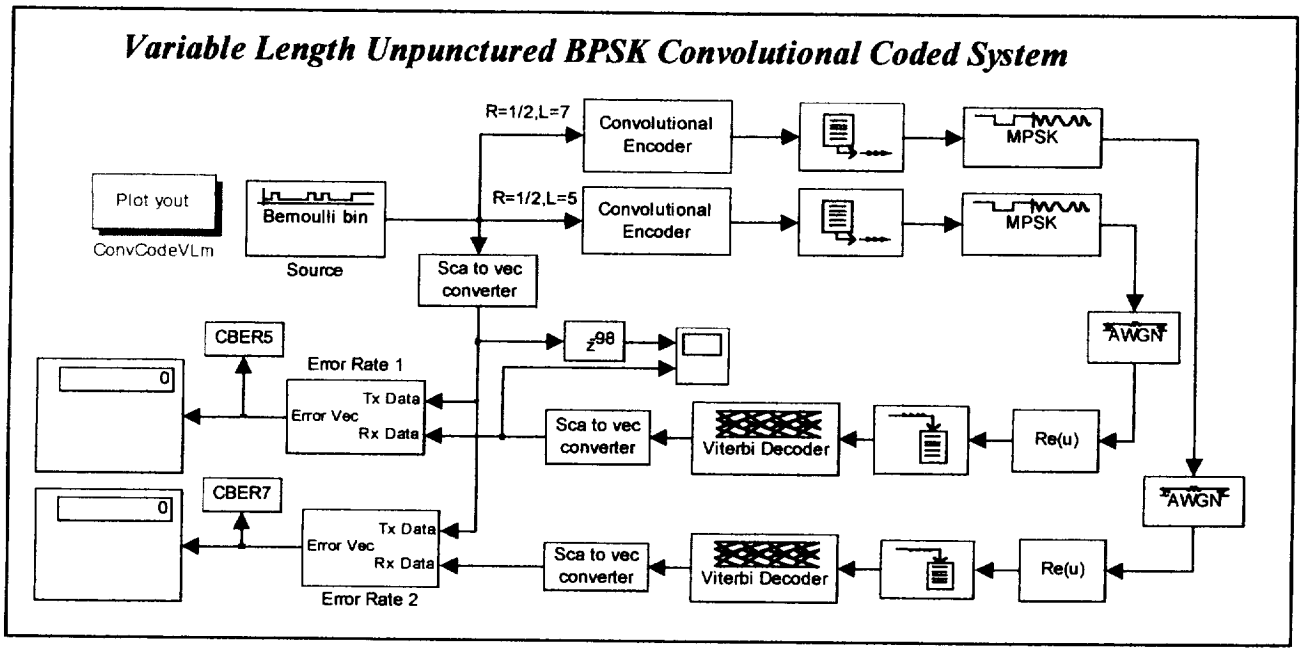

Fig. 16: Variable Constraint Length Convolutional Coding

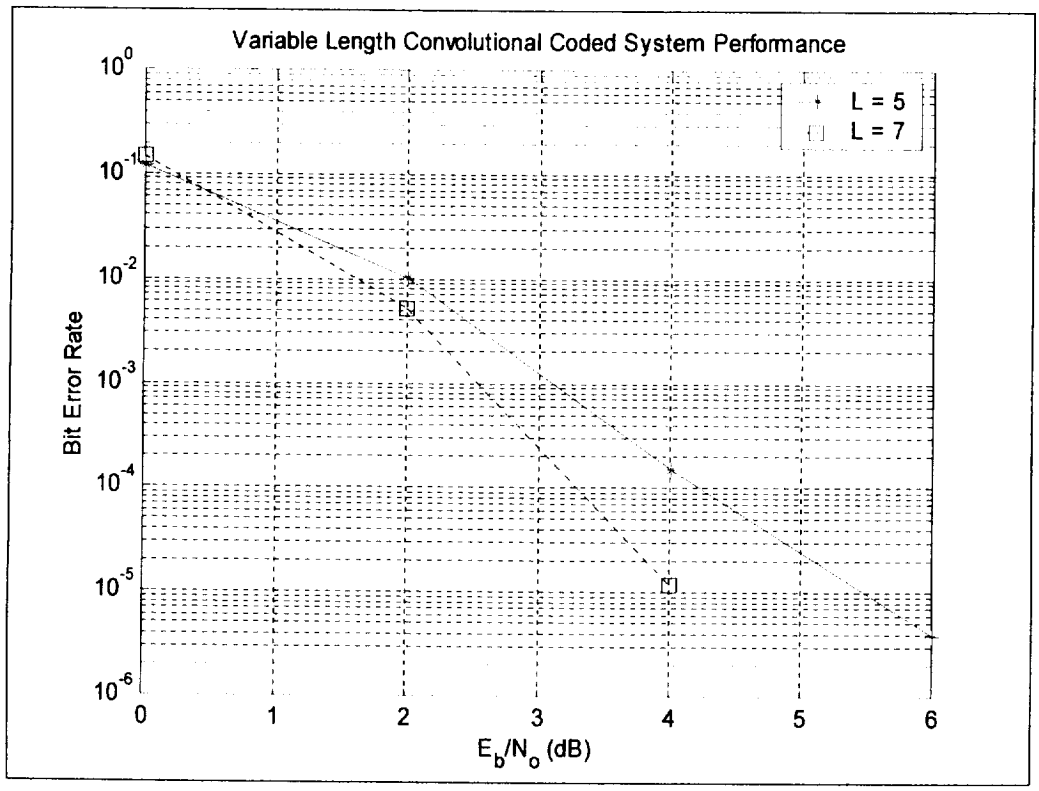

Fig. 17: BER Performance of Convolutional Coded System with Variable Constraint Lengths.

Figure 18 is used to study the feasibility of multiplexing punctured convolutional coded system similar to that shown in Fig. 8. It shows a two channel system with uplink and downlink channels. By having separate, we manipulate the properties of each link since the characteristics of uplink and downlink channels in a satellite communication system may have different.

To obtain a more robust coding technique, it is possible to combine different rates and constraint lengths, thereby verifying the effect of rate change and constraint length change simultaneously. The motivation will be to simultaneously explore the effect of variable constraint length and combinations of variable rates. Since it is possible that a component or subsystem of the AATT can be operating at a different rate, our objective is to study the effect of different rates or constraint lengths combined into one model.

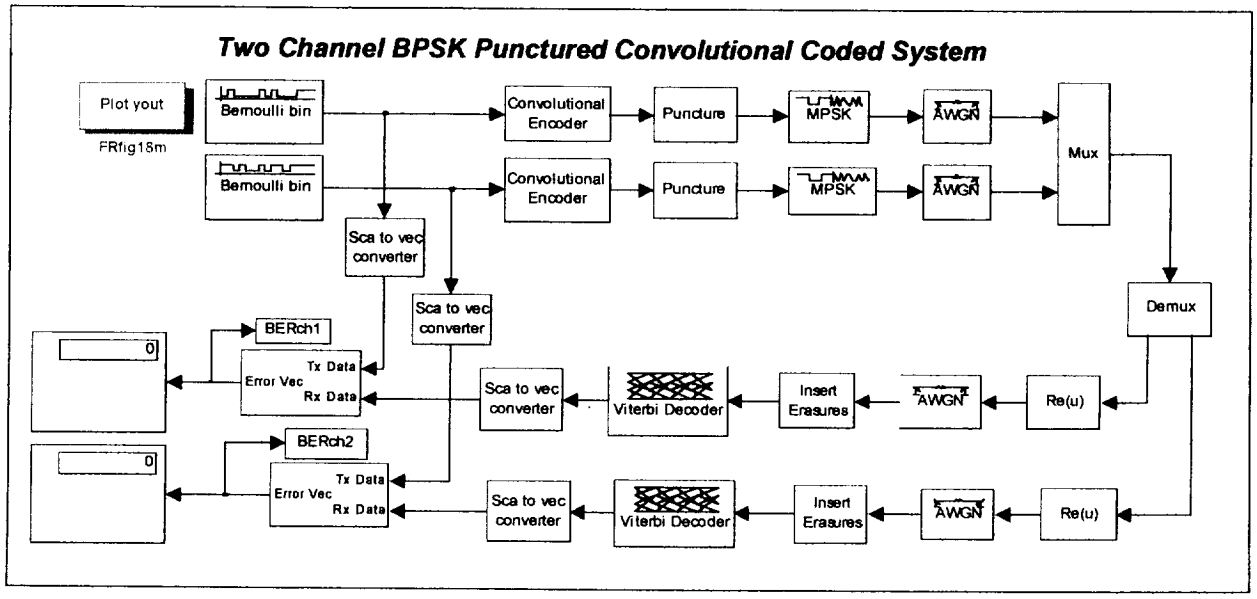

Fig. 18: Two-Channel Punctured Convolutional Coding, Rate 3/4, Constraint Length 7.

2. *Reed-Solomon Coded Communication System*

Because of the popularity of Reed-Solomon (RS) coding in satellite communications, the performance of communication systems applying Reed-Solomon code was also studied. A sample model is shown in Fig. 19 for a single channel Reed-Solomon coding. This model was simulated and the results compared to uncoded system. Performance result shown in Fig. 20 displays an interesting behavior. Effect of RS coding is insignificant for small values of E_b/N_0, specifically when E_b/N_0 is less that 3 dB. However, when E_b/N_0 is large, the performance of RS coding is better than that of uncoded RS system.

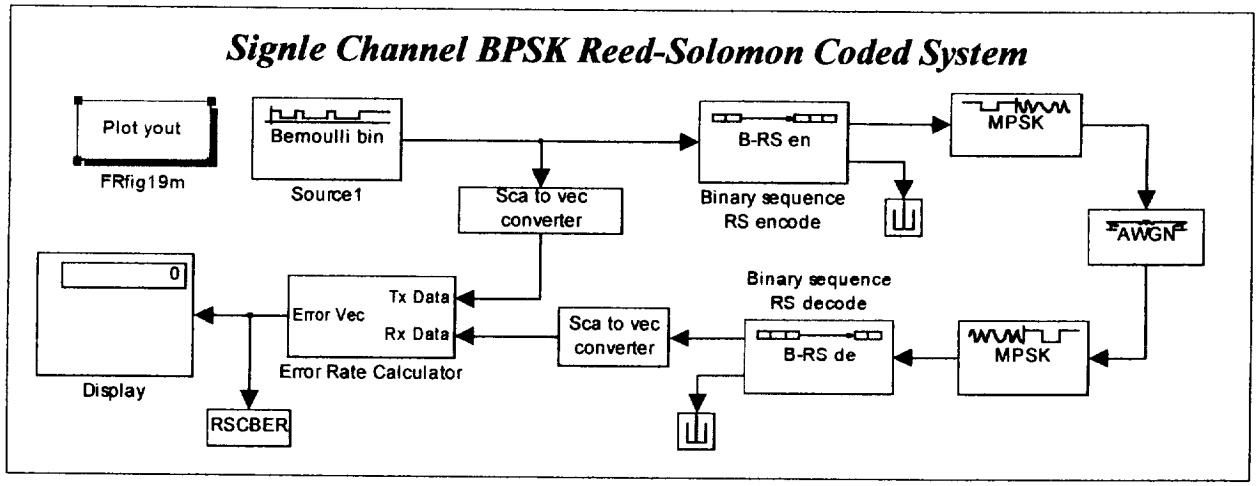

Fig. 19: Single Channel BPSK Reed-Solomon Coded System.

It is perhaps important to mention that the computation time for this model is very long. It takes a very long time for this model to run; hence, the result shown in Fig. 20 is truncated. The reason why this model takes a very long time is still unknown to us. Because of the excessive simulation time for the RS coding, most of the models developed for this coding scheme were suspended.

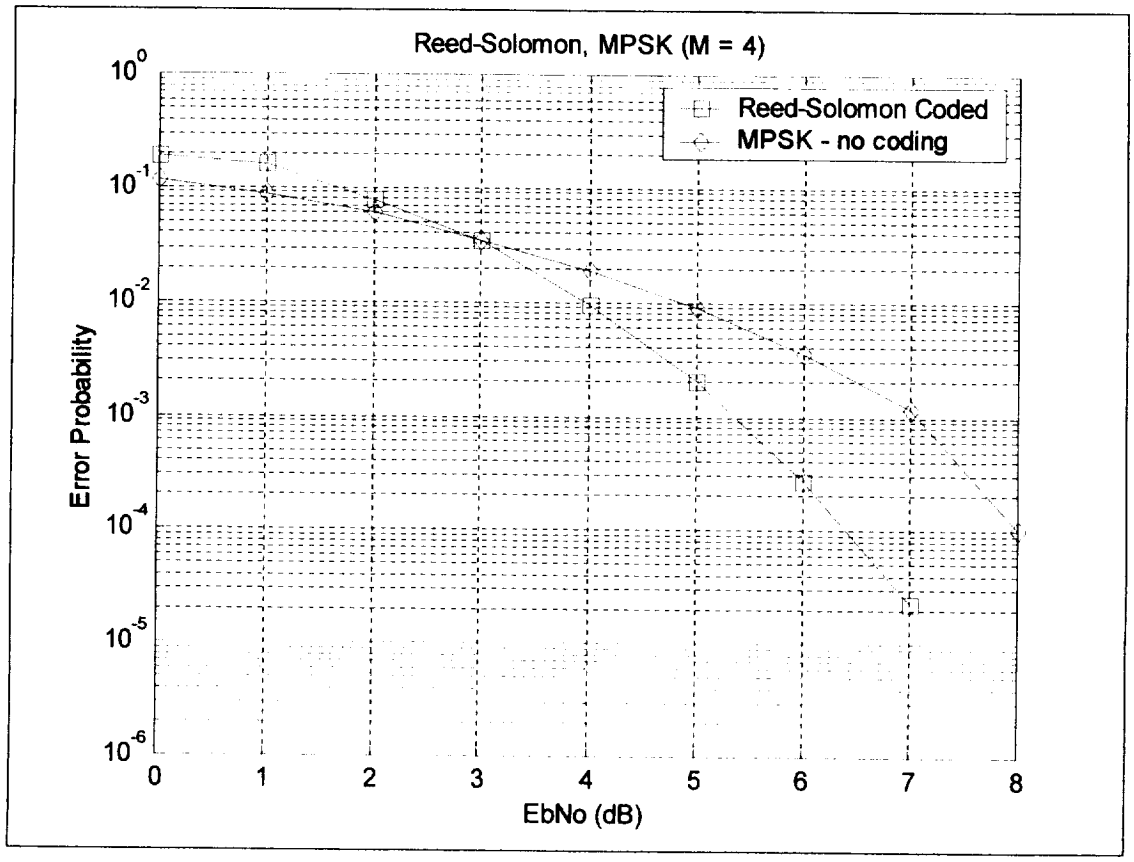

Fig. 20: Comparison of Uncoded and Reed-Solomon Coded System.

3. Multiple Access Capability

The next task was to study the feasibility of applying Multiple Access protocol. The multiple access techniques that were considered include Time Division Multiple Access (TDMA), Frequency Division Multiple Access (FDMA), and Code Division Multiple Access (CDMA). A sample model for frequency hopping multiple access technique is shown in Fig. 21.

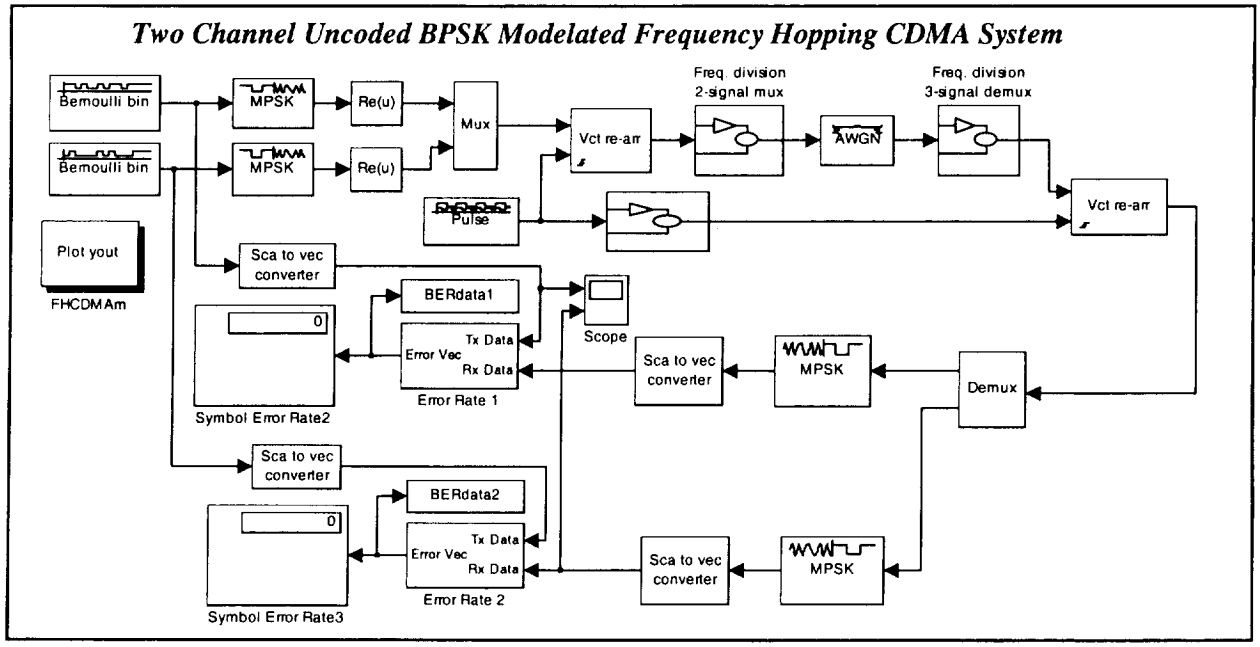

Fig. 21: Model of Frequency Hopping Multiple Access Techniques.

Unfortunately, SIMULINK simulation of multiple access techniques is troublesome. All multiple access techniques seem to generate fractional delays that are not resolvable at the receiver. This means that the transmitted signal and the received signal cannot be synchronized. Hence, high error probability is obtained in each simulation. After several attempts to resolve this problem, it became apparent that it is a software problem independent of the model. We believe that this problem is a defect in the software and should be resolved by the manufacturer [3]. The manufacturer has been notified of this problem. There are many multiple access models configured for this project, but it will not be meaningful to include them here since we do not have a corresponding result. We are hopeful that this problem could be resolved in the next version of the software.

C. System Definition of AATT Communication Scenarios

In this task, we focused on defining the communication channel scenarios. Beginning with the conventional Air Traffic communication scenario shown in Fig. A1 [8], conceptual communication links were suggested. This is shown in Fig. A2, Appendix A. The idea was to identify all possible communication scenarios that could arise in this project showing the integration of the ground stations, ships, aircrafts, satellites, control centers and mobile networks. Please note that in these definitions system overlay was taken into consideration, since most of the existing communications infrastructure must be utilized.

By considering all the possible communication links, probable AATT channels shown in Fig. 22 were identified. It is the simplification of the conceptual AATT links shown in Fig. A2, with number attached to the probable links.

From this scenario, we can identify the following communication links scenarios.

1. Satellite-to-Ground Earth Station Communication Link
    1. Also contains Satellite-to-Gateway communication

2. Aircraft-to-Control Center Communication Link
    2. Also includes the Aircraft-to-Radio Tower Link

3. Aircraft-to-Aircraft Communication Link

4. Satellite-to-Aircraft Communication Link

5. Satellite-to-Satellite (Inter-satellite) Communication Link
    - Geosynchronous-to-Low Earth Orbit
    - Geosynchronous-to-Medium Earth Orbit
    - Medium Earth Orbit-to-Low Earth Orbit

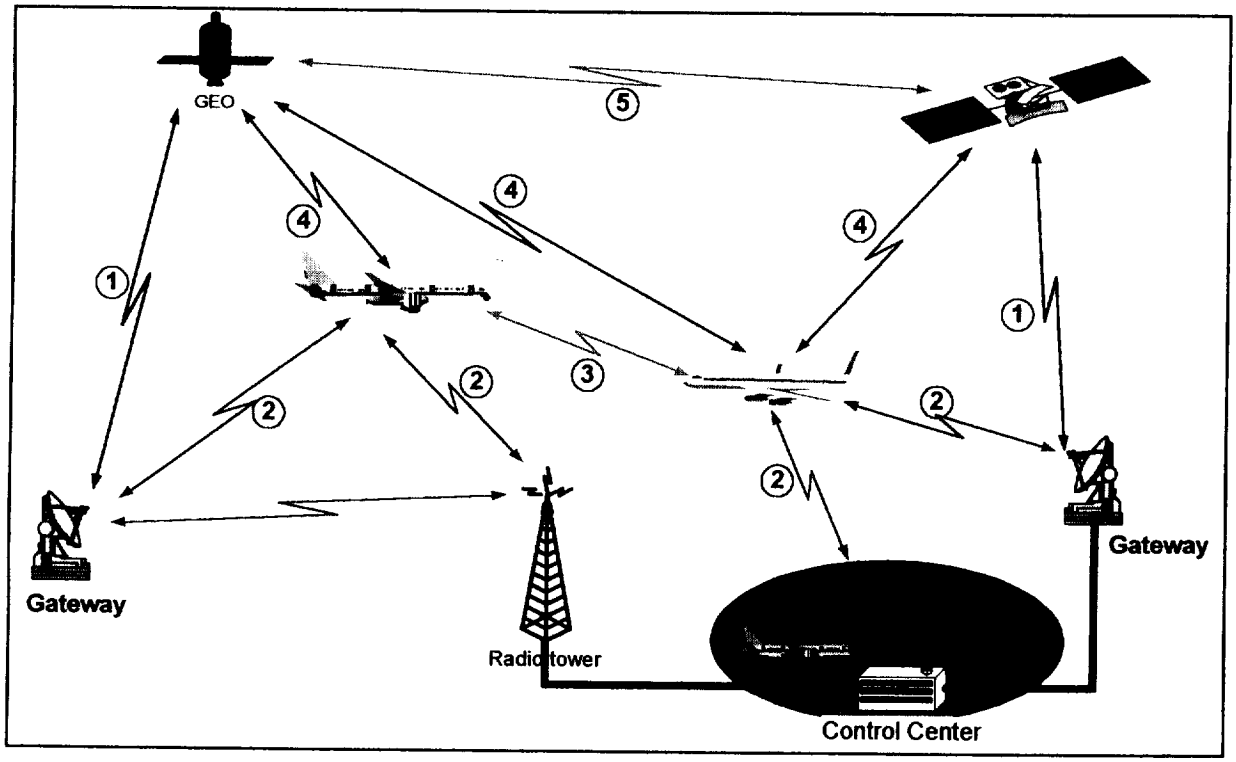

Fig. 22: Schematic of Probable AATT Communication Links.

The individual links of Fig. 22 are illustrated in Appendix B. Please note that the technology to realize some of these links is currently not available or is seriously limited. For example, the communication between Aircraft and Airport Tower is limited to a radius of 25 miles. The communication between Satellite and Aircraft is non-existent, except for navigational or positional information from the Global Positional Satellite. Aircraft and Aircraft cannot communicate directly unless they are very close to one another.

Thus, after some reexamination of these links, taking into consideration conditions for practical implementation, the links were redefined and reduced to two primary end-to-end links. The two primary links are identified as the GEO Communication Link and the LEO Communication Link. These two are analyzed in details in the next task.

D. System Analysis of Identified AATT Communication Links

The objective in this task is to analyze in detail the two primary links defined above providing complete end-to-end communication systems architectural, link parameter definitions and analysis, and link budget calculation. The system parameters for each of the links were determined and analyzed.

First, all applicable communication link parameters must be defined or specified. In consultation with the NASA research team, the most probable communication parameters were chosen. The first primary link, GEO Communication Link, is shown in Fig. 23 and the corresponding link parameters are shown in Table 2.

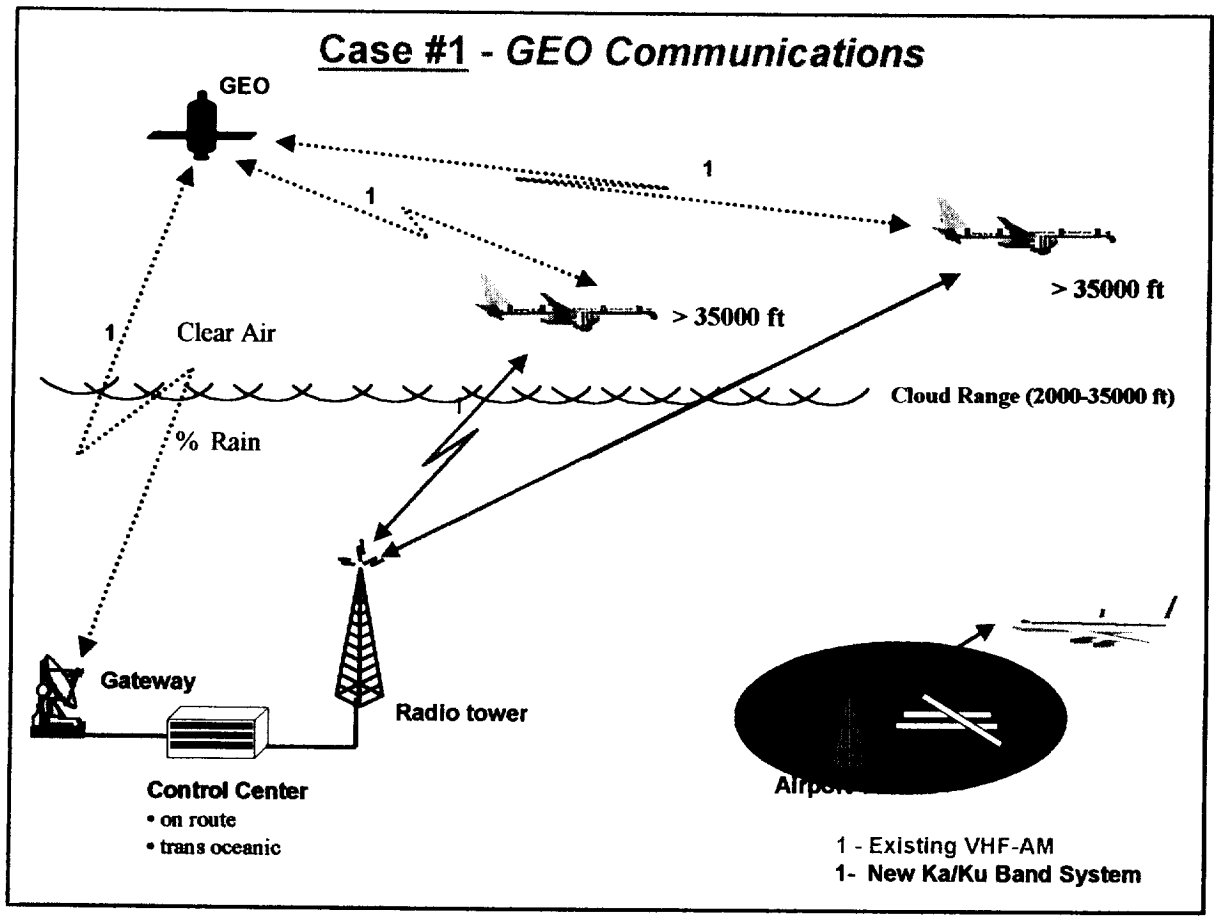

Fig. 23: GEO Communication Link Scenarios.

In this link scenario, the GEO satellite can directly communicate with the Control Center Gateway and the Aircraft above the cloud range. However, it cannot communicate with the

Radio Tower or with the Airport Tower. Airplanes can communicate with the Radio Tower but not with each other or the Airport Tower, except when they are within range of the airport. Please note that the mechanism for GEO communicating directly with the airplane is currently not available. Also, note that although current communication uses VHF or UHF signal, but the analysis in this project assumes operation at Ka-band.

In the link budget analysis, variation in the radio link is usually a big factor. The calculation of available Carrier-to-Noise power ratio (C/N_O) and the corresponding margins are very important. These parameters depend on characteristics of the radio terminals (i.e., transmitters, receivers, antennas), the characteristics of the propagation medium, the interference and noise properties. Central to link budget calculation is noise, which is generated from different sources in the link. For example, noise is generated by active electron devices usually referred to as intermodulation noise or LNA noise; noise is inherent in the motion of electrons; noise is associated with system temperatures; and noise is received from outer space as in AWGN, rain fade, absorption, refraction and many more. Among these noise factors, rain fade is the most troublesome for satellite communications operating in the Ka-band. This is because as the frequency increases above Ku-band, the severity of impairment also increases. Attenuation caused by rain along a signal path represents one of the dominant causes of fading in a satellite communication link [9], [10]. Rain attenuation is a function of frequency, elevation angle, polarization angle, rain intensity, raindrop size distribution and raindrop temperature [11]. It is the interference caused by raindrops on electromagnetic signals traveling through the atmosphere. When this phenomenon occurs, the transmission is weakened by absorption and scattering of the radio wave. However, results from Ka-band studies [2] have shown that mitigation and compensation techniques must be incorporated in system design to operate at or above Ka-band. Hence, analysis of link budget must consider the effects of these noise sources.

The second primary link, the LEO communication channel, is shown in Fig. 24. This link is identical to the GEO link in many ways. The only difference is that the GEO satellite is replaced with a LEO satellite and their reference distances are different. We have chosen the parameters to be the same since many of the operational data for LEO satellite is not readily available. When real practical data is available, the parameters can be easily modified.

The corresponding parameters for the LEO Communication Link scenarios are given in Table 3. These numbers were chosen based on experience and were correlated with known GEO communication link parameters.

Table 2: GEO Communications Link Parameters

GEO Communication Link Parameters

Case 1: Earth Station (Control Center) to GEO Satellite to Aircraft

Specifications for Ka-band (Uplink at 30 GHz and Downlink at 20 GHz)

•Ground Station System	
• Antenna Diameter (Tx & Rx)	- 2.5 Meters (GEO tracking)
• Power RF	- 60 Watts
• Noise Figure	- 3.0 dB
• Bandwidth	- 300 MHz
• Modulation	- BPSK with Convolutional Coding
• Access Technique	- TDMA/CDMA
• Satellite (GEO)	
• Antenna Diameter (Rx)	- 2.0 Meters
• Antenna Diameter (Tx)	- 1.5 Meters
• Power	- 40 Watts
• Noise Figure	- 3.0 dB
• Satellite Transponder Loss	- 3.0 dB
• Aircraft	
• Antenna Gain (Tx & Rx)	- 1.5 dB
• Noise Figure	- 3.0 dB
• Power	- 0.25 watts
• Bandwidth	- 2.0 MHz

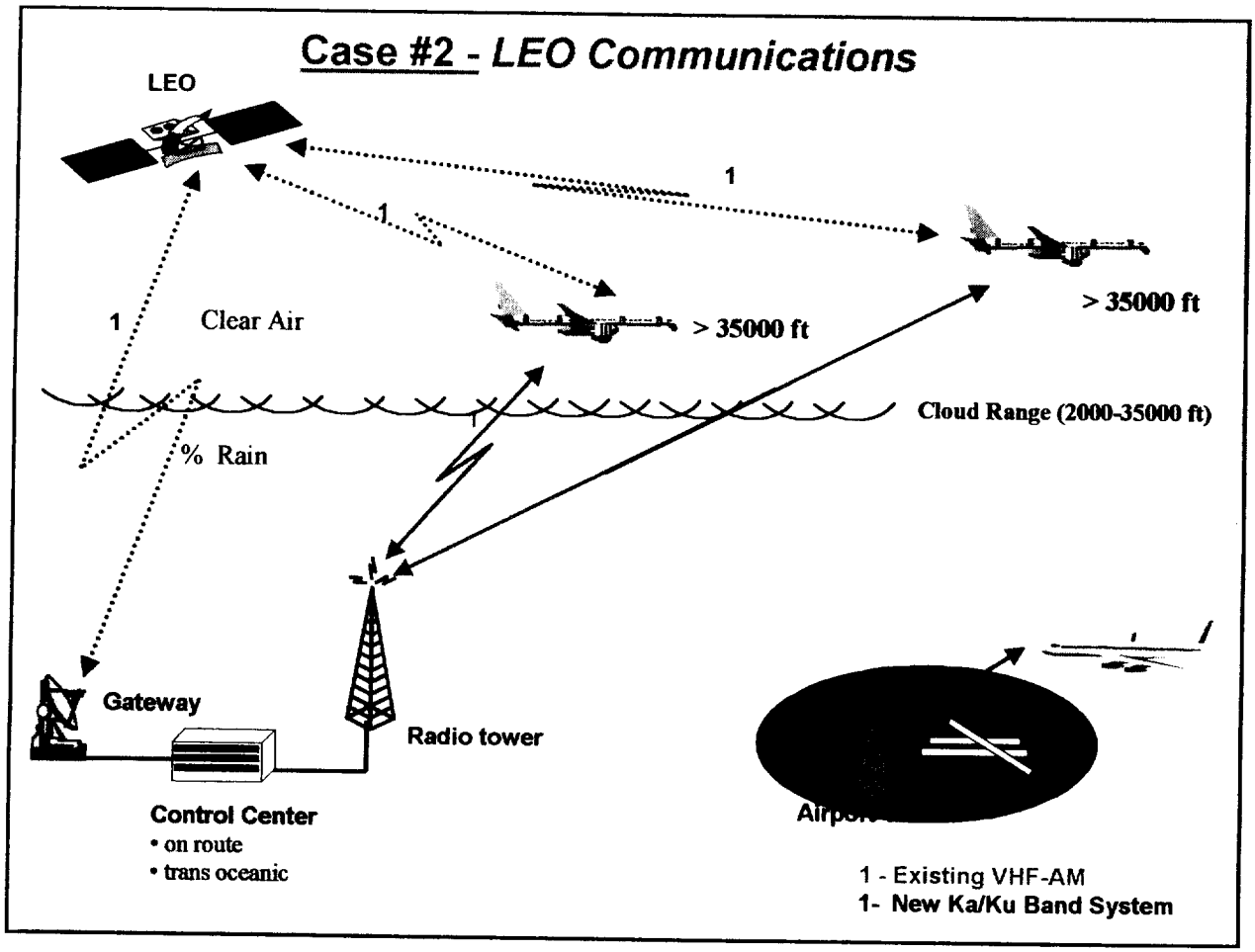

Fig. 24: LEO Communication Link Scenarios.

Table 3: LEO Communication Link Parameters

LEO Communication Link Parameters

Case 2: Earth Station (Control Center) to LEO Satellite to Aircraft

Specifications for Ka-band (Uplink at 30 GHz and Downlink at 20 GHz)

•Ground Station System	
• Antenna Diameter (Tx & Rx)	- 2.5 Meters (non tracking)
• Power RF	- 60 Watts
• Noise Figure	- 3.0 dB
• Bandwidth	- 300 MHz
• Modulation	- BPSK with Convolutional Coding
• Access Technique	- TDMA/CDMA
• Satellite (LEO)	
• Antenna Diameter (Rx Tracking)	- 2.0 Meters
• Antenna Diameter (Tx Tracking)	- 1.5 Meters
• Power	- 40 Watts
• Noise Figure	- 3.0 dB
• Satellite Transponder	- 3.0 dB
• Aircraft	
• Antenna Gain (Tx & Rx)	- 1.5 dB
• Noise Figure	- 3.0 dB
• Power	- 0.25 watts
• Bandwidth	- 2.0 MHz

D. Link Budget Analysis

Using the parameters specified in Tables 2 and 3, the link budget was calculated for the two primary links. Initially, the link budget was computed in both MATHCAD and MATLAB. However, this process is tedious and time consuming since the program is modified each time a change is made. It was then suggested by Dr. Acosta that a more automated method of computing the link budget be investigated. This suggestion led to the development of a graphic user interface (GUI) program for the link budget analysis. Since the link budget is always required in any space communication, it will be prudent to automate the computation.

The GUI program is developed in MATLAB. The program offers a unique set of graphical-user interfaced-based tools designed to enable easy computation of the link budget. Each routine or interface is interactive and is built for easy selection and straightforward computation without programming.

This program is activated by typing ***"Link_Program"*** at the MATLAB prompt. This invokes the first interface shown in Fig. 25. From the interface, you can select the ***Forward Link, Reverse Link, Antenna Parameters or BER Performance.*** In addition, a particular communication link scenario or modulation scheme can be selected. Since we are mainly concerned with binary signal, the result for BPSK and QPSK is the same.

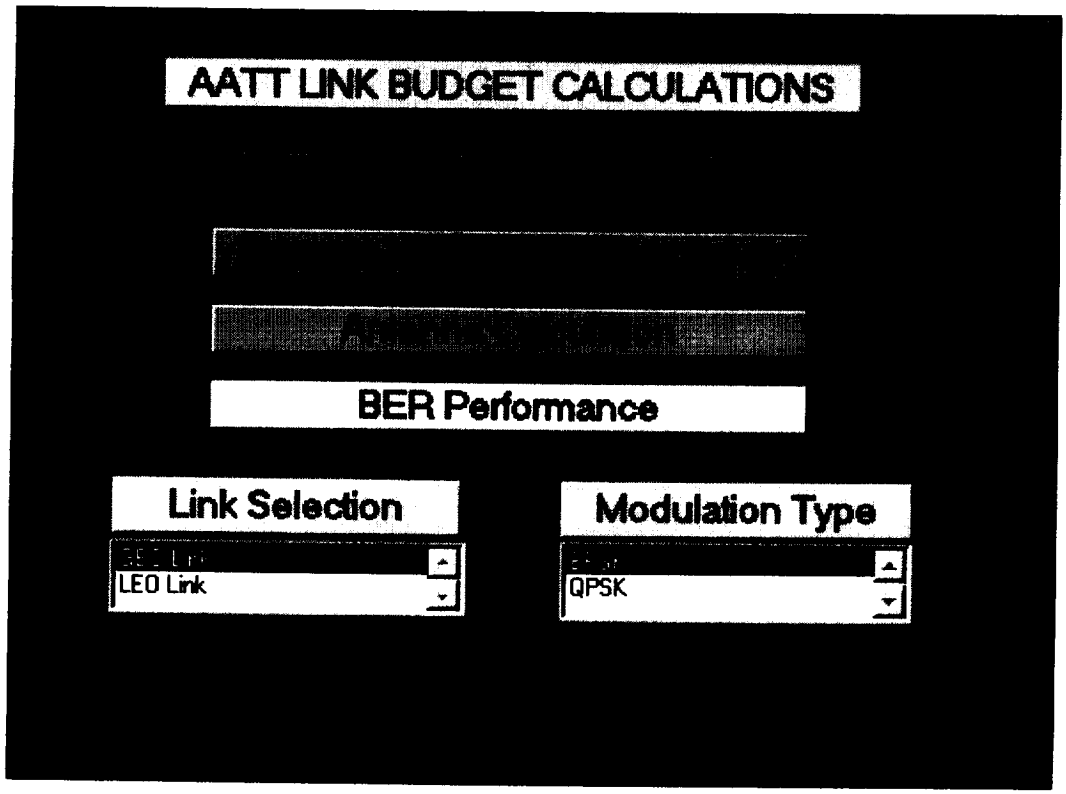

Fig. 25: First GUI Interface for Link Budget Calculations

Selecting an item from the above interface will either generate another interface for data input for that selected item or compute the result in the case of BER performance. For example, selecting the Forward Link will bring up the interface shown in Fig. 26 for the Forward Link input parameters.

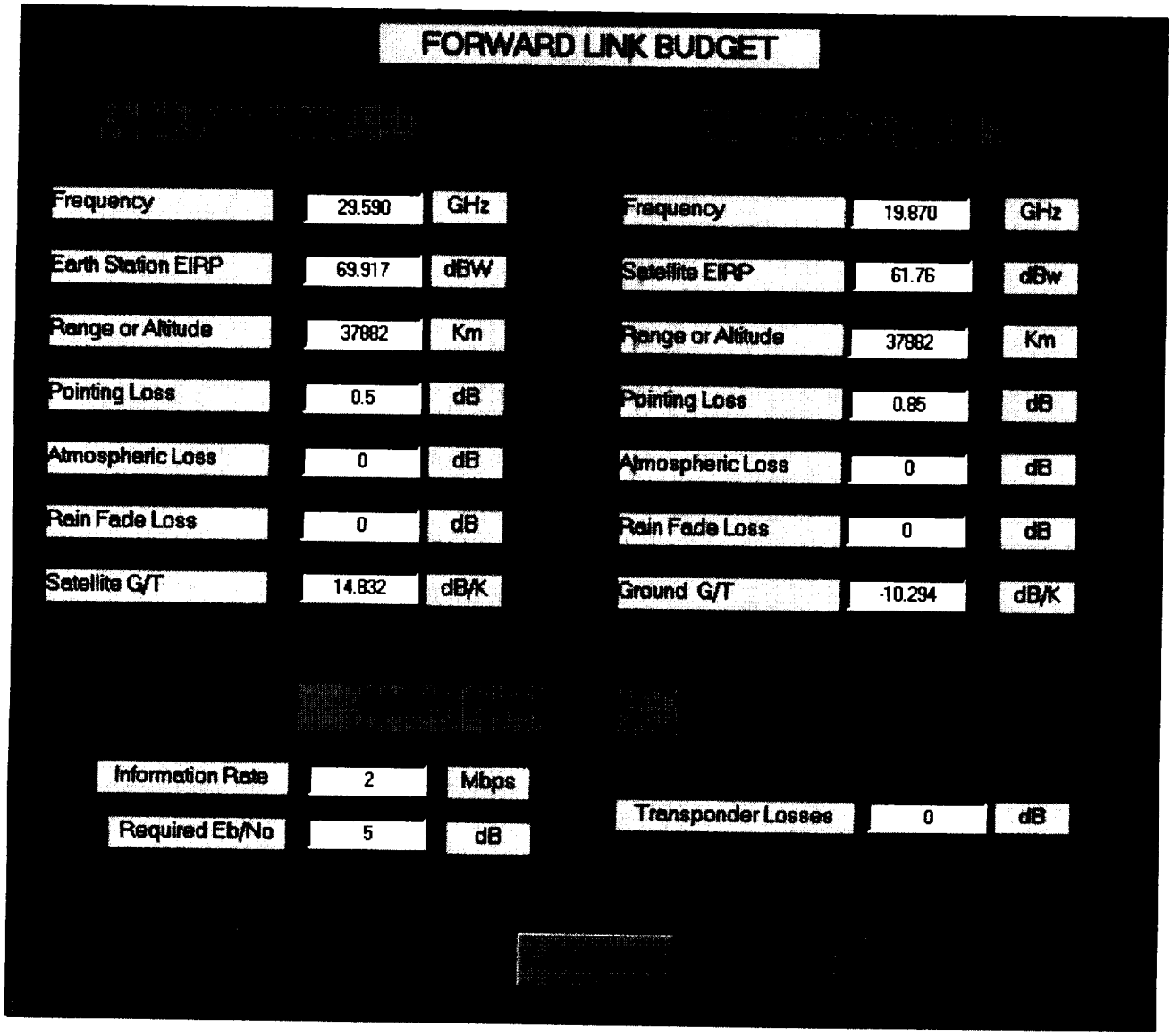

Fig. 26: Data Input Interface for Forward Link Budget Calculation

After the input of the necessary parameters, then the link budget is calculated by single clicking the "CALCULATE" button. For example, the input parameters for the Forward Link of the GEO communication channel are shown in Fig. 26. Activating the "CALCULATE" button will generate the link budget parameters shown in Fig. 27.
In this window, all the needed link budget parameters are shown. The margin and the BER are also shown for the input data of Fig. 26. If one is studying the effect of a particular

parameter, a simple change in Fig. 26 can be made and the link budget regenerated without the need to change the program.

Notice that in Fig. 27 the coded and uncoded BER is also listed. The coded BER is generated by using the calculated E_b/N_0 in a polynomial equation. However, the uncoded BER is calculated from the link budget equations. This is necessary in order to compare the coding gain in the link budget analysis.

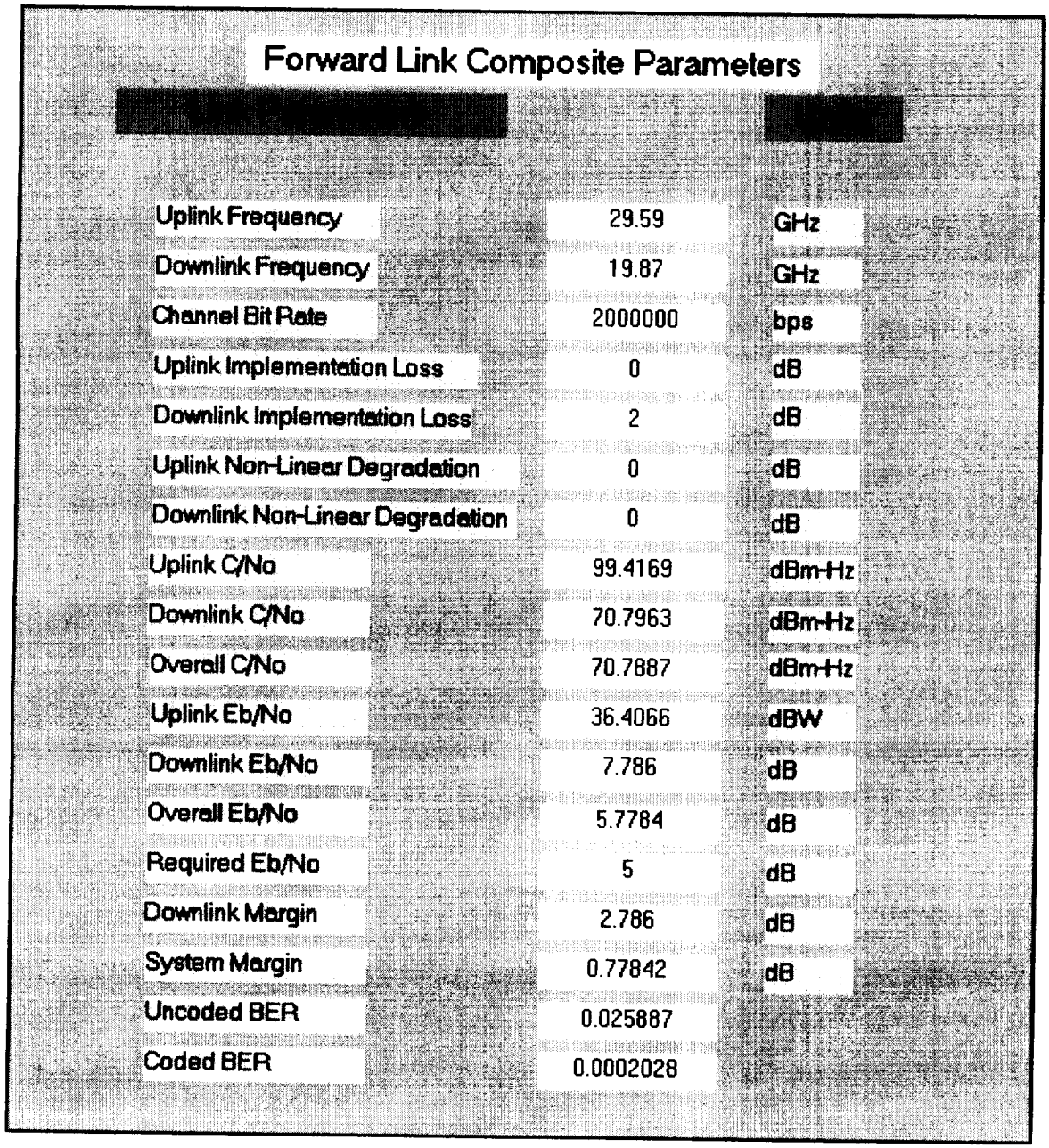

Forward Link Composite Parameters

Uplink Frequency	29.59	GHz
Downlink Frequency	19.87	GHz
Channel Bit Rate	2000000	bps
Uplink Implementation Loss	0	dB
Downlink Implementation Loss	2	dB
Uplink Non-Linear Degradation	0	dB
Downlink Non-Linear Degradation	0	dB
Uplink C/No	99.4169	dBm-Hz
Downlink C/No	70.7963	dBm-Hz
Overall C/No	70.7887	dBm-Hz
Uplink Eb/No	36.4066	dBW
Downlink Eb/No	7.786	dB
Overall Eb/No	5.7784	dB
Required Eb/No	5	dB
Downlink Margin	2.786	dB
System Margin	0.77842	dB
Uncoded BER	0.025887	
Coded BER	0.0002028	

Fig. 27: Forward Link Budget for GEO Communications

The above operations can be repeated for the Reverse Link Budget calculations with the corresponding interface and link budget parameters shown in Figs. 28 and 29, respectively.

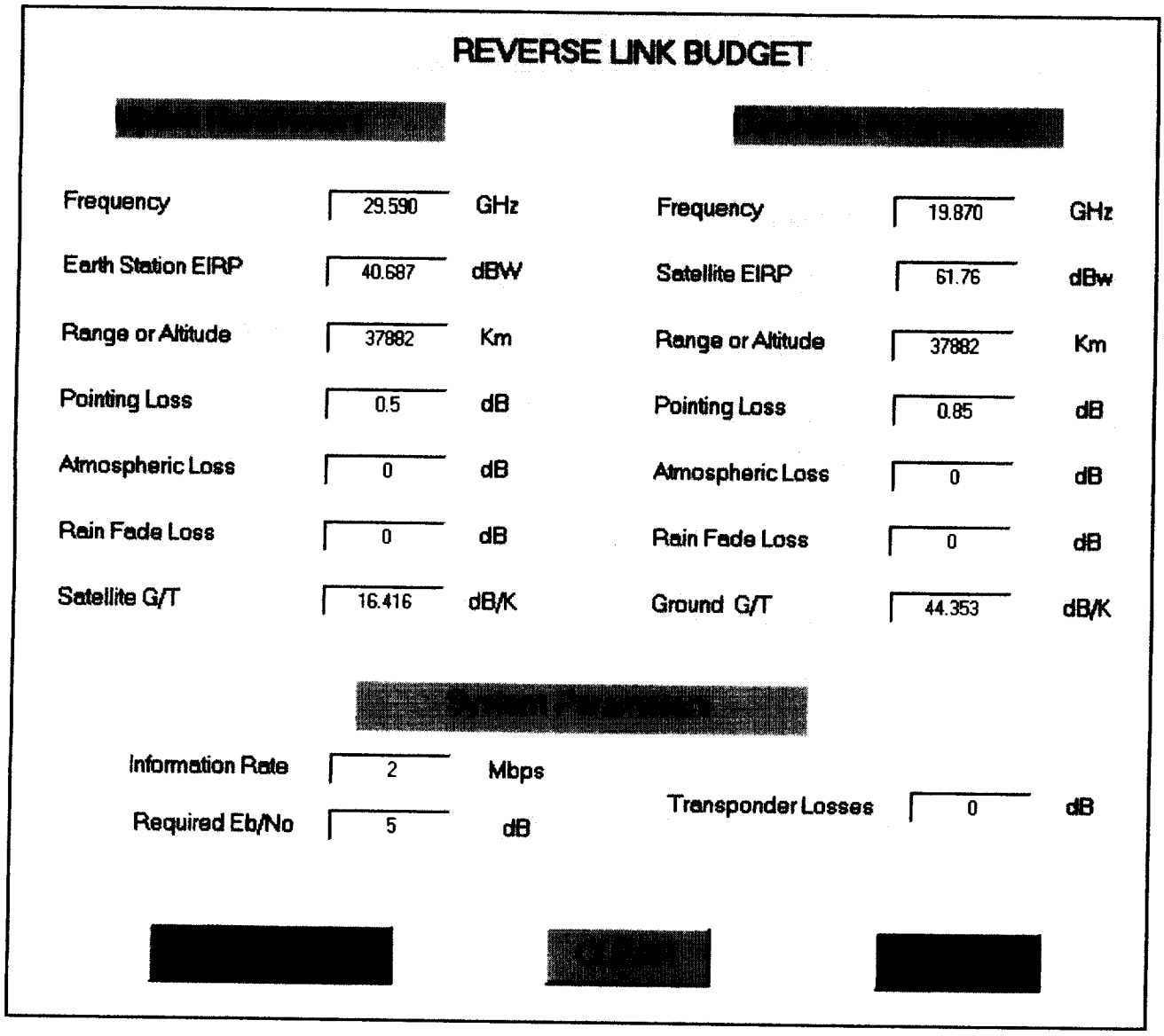

Fig. 28: Data Input Interface for Reverse Link Budget Calculation

Reverse Link Composite Parameters

Uplink Frequency	29.59	GHz
Downlink Frequency	19.87	GHz
Channel Bit Rate	2000000	bps
Uplink Implementation Loss	0	dB
Downlink Implementation Loss	2	dB
Uplink Non-Linear Degradation	0	dB
Downlink Non-Linear Degradation	0	dB
Uplink C/No	71.7709	dBm-Hz
Downlink C/No	112.3771	dBm-Hz
Effective C/No	70.7209	dBm-Hz
Overall C/No	70.7206	dBm-Hz
Uplink Eb/No	8.7606	dBW
Downlink Eb/No	49.3668	dB
Overall Eb/No	5.7103	dB
Required Eb/No	5	dB
Downlink Margin	44.3668	dB
System Margin	0.71028	dB
Uncoded BER	0.026815	
Coded BER	0.00023717	

Fig. 29: Reverse Link Budget for GEO Communications

It is important to mention that the Forward and Reverse Link budget shown on Figs. 27 and 29 are the CLEAR SKY link budget. Hence, the uplink, downlink and system margins are CLEAR SKY margins. The effects of propagation anomalies or fade are not included.

The Antenna Parameters can be calculated in a similar manner with the input interface shown in Fig. 30. The antenna parameter may be required as an input for the link budget. Fig. 30 interface is used to compute the Antenna EIRP or Antenna G/T. When the "CALCULATE" button is activated, the EIRP and the G/T parameters are calculated and displayed on the same window as shown in Fig. 31.

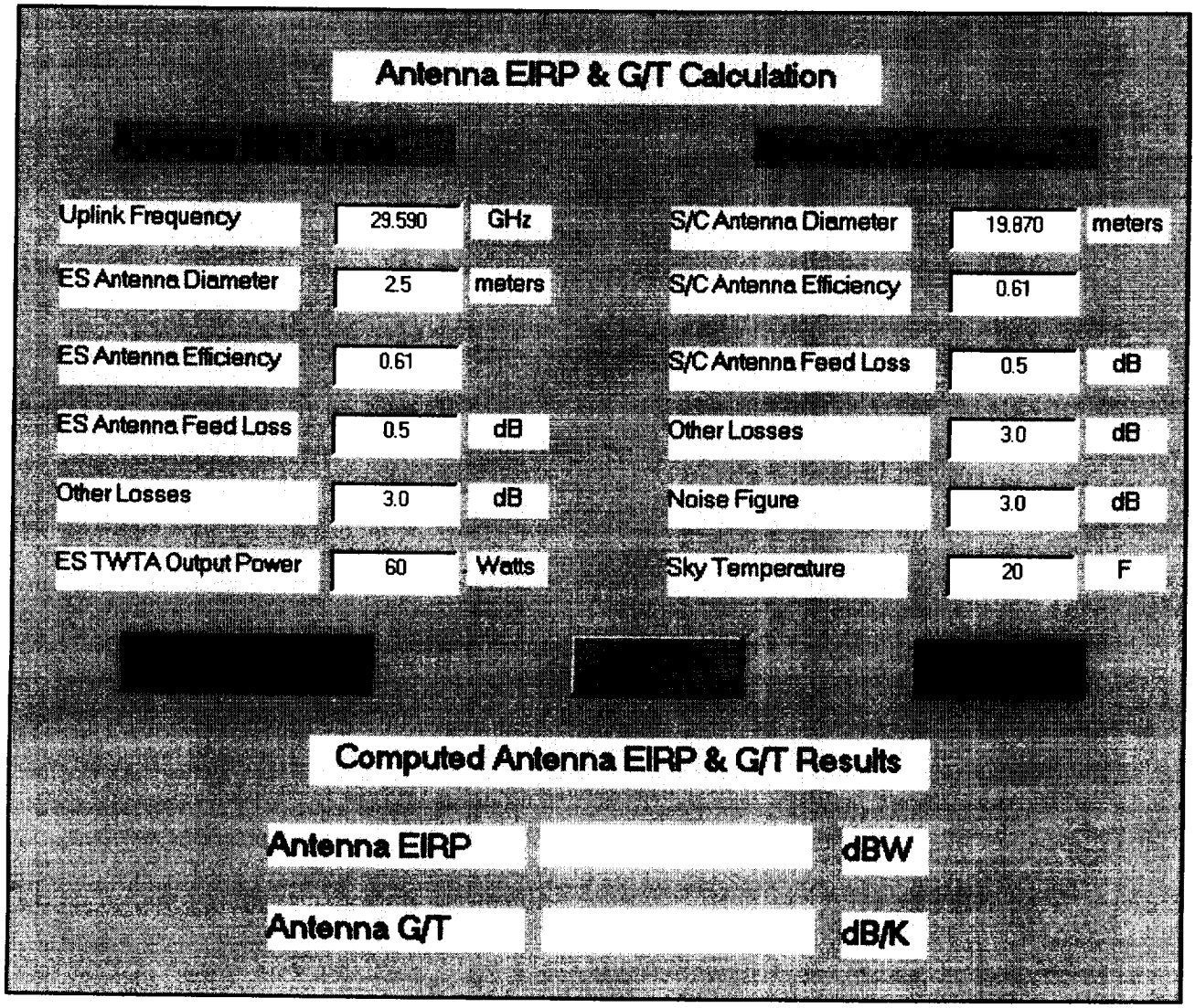

Fig. 30: Data Input Interface for Antenna Parameter Calculations

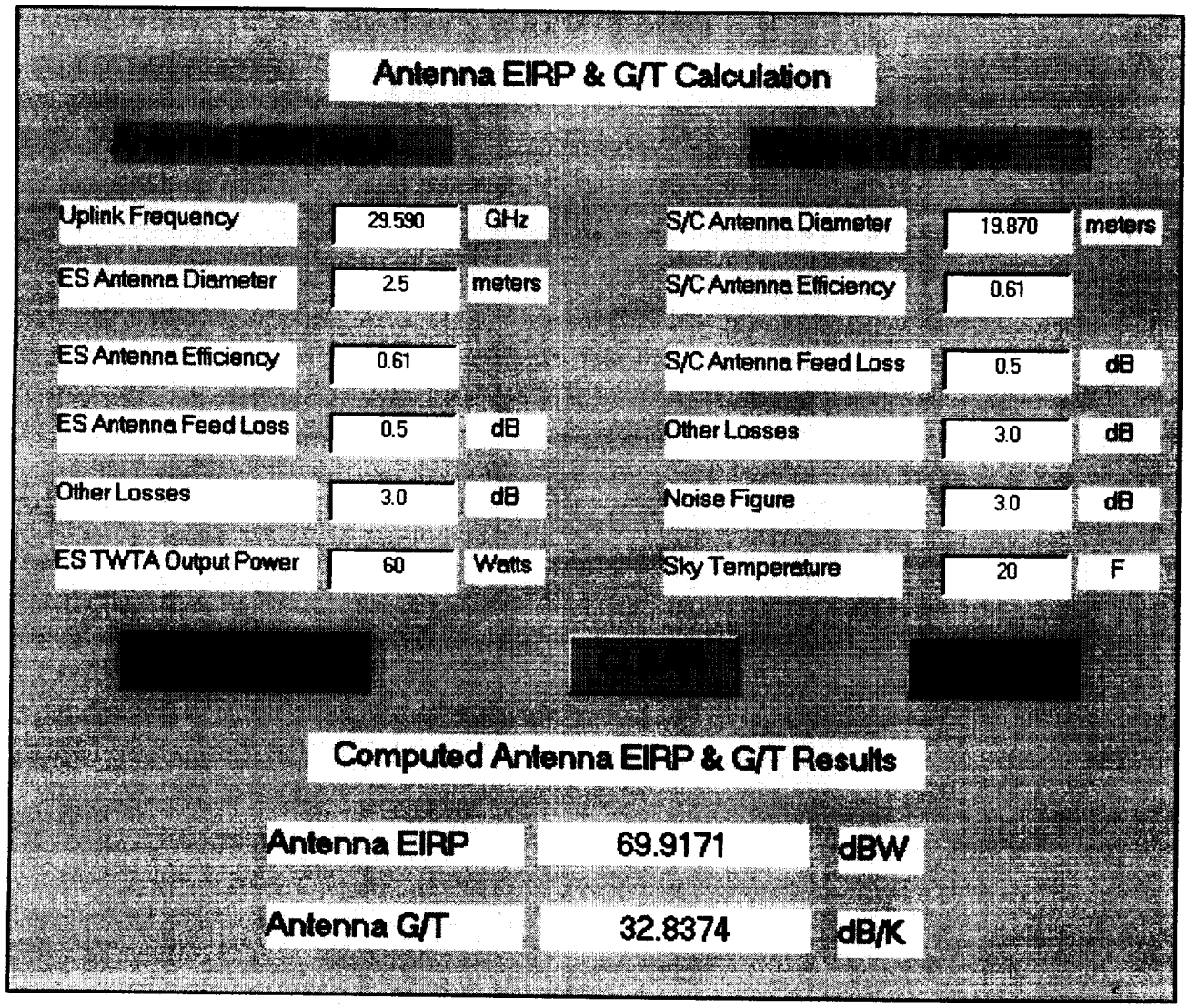

Fig. 31: Antenna Parameter Calculations

The last option in Fig. 25 is the BER Performance button. Selecting this option will plot the BER performance curve as a function of the E_b/N_0 for both BPSK and QPSK. This is shown in Fig. 32. It is the expected theoretical BER, which can be used to validate the coded, or uncoded BER listed in Fig. 27 or 29, with reference to a particular value of E_b/N_0. This plot can also be produced by selecting either the BPSK or the QPSK from the modulation type window of Fig. 25.

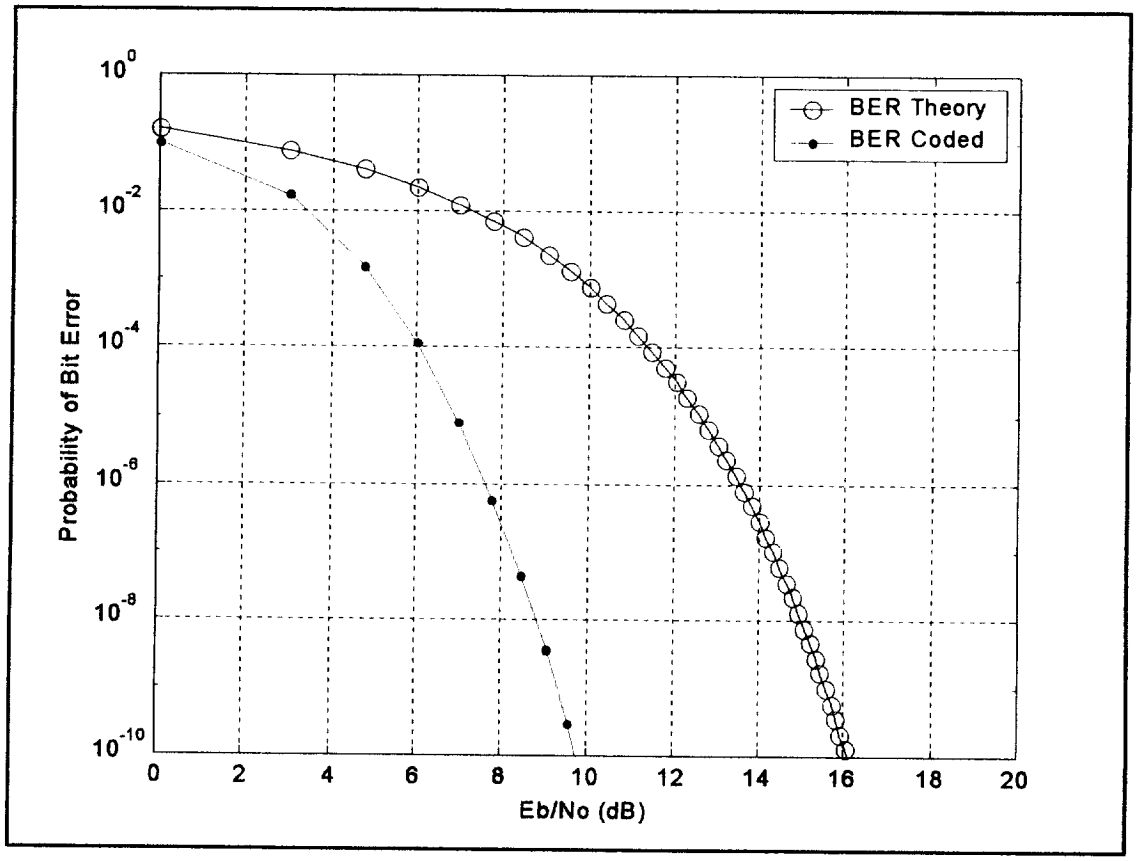

Fig. 32: Coded and Uncoded BER Performance Curve.

SUMMARY AND CONCLUSIONS

In this report, we have described the communication systems architecture for the AATT project. Different communication scenarios were proposed and analyzed. The proposed communication scenarios were modeled and simulated in MATHCAD and in MATLAB SIMULINK. We have compared the simulation results with theoretical values and found a close match. It was observed that due to lack of specific definition for system parameters, parameters that are more practical could not be used.

The identified communication link scenarios are the most probable based on current technology. Further work to investigate the effect of propagation on system availability is recommended. We believe that continuation of this project will lead to the following specific contributions:

1. Investigate the effects of propagation anomalies on system availability. This implies that the propagation effects and system parameters that could degrade performance will be identified, analyzed, and incorporated into the overall performance analysis.

2. Given the identified communication link scenarios, investigate the specific effect of rain fade in system performance. Based on results, suggest methods for fade mitigation.

3. Simulate the statistical behavior of the end-to-end system performance incorporating as many variables as possible.

4. The availability of significantly improved software program for computing the link budget parameters for different communications link scenarios.

ACKNOWLEDGMENTS

The work described in this report was carried out at The University of Akron and NASA Glenn Research Center (GRC), under contract with NASA Space Communications Division at GRC, Cleveland. The author is indebted to Dr. Roberto Acosta, Project Development and Integration Branch, NASA GRC, for working very closely with me in this project. In addition to his personal involvement, he made excellent suggestions that made the task less tasking. My gratitude also goes to other team members from NASA particularly Sandy Johnson and Walber Feliciano who were also actively involved in the project. Many thanks to the AATT Project Manager, Konstationos Martzaklis, for making the funds available for this project.

REFERENCE

[1]. Lockheed Martin Aeronautical Systems, *"Free Flight Satellite Communication Study, NASA Advanced Air Transportation Technologies,"* Final Report, Free Flight Satellite Communication Study, NASA Glenn Research Center, May 1998.

[2]. R. J. Acosta, *eta. al.*, "Advanced Communications Technology Satellite (ACTS): Four Year System Performance," *IEEE Journal of Selected Area,* JSAC-17, no. 2, February 1999.

[3]. Mathworks Inc., 24 Prime Park Way, Natick, MA 01760, http://www.mathworks.com

[4]. D. Haccoun and G. Begin, "High-Rate Punctured Convolutional Codes for Viterbi and Sequential Decoding," *IEEE Journal of Communications, vol. Comm-37, no. 11, pp. 1113-1125, Nov. 1989.*

[5]. D. Haccoun and G. Begin, "High-Rate Punctured Convolutional Codes: Structure, Properties and Construction Techniques," *IEEE Journal of Communications, vol. Comm-37, no. 12, pp. 1381-1385, Nov. 1989.*

[6]. Y. Yasuda, K. Kashiki and Y. Hirata, "High-Rate Punctured Convolutional Codes for Soft Decision Viterbi Decoding," *IEEE Journal of Communications, vol. Comm-32, no. 3, pp. 315-318, Mar. 1984.*

[7]. NASA Lewis Research Center, *Systems Handbook - Advanced Communications Technology Satellite*, Technical Report TM-101490.

[8]. R. J. Kerczewski, "Aeronautical Communications System Architecture," Satellite Network and Architecture Branch, NASA Glenn Research Center, July 13, 1999.

[9]. R. J. Acosta, "Rain Fade Compensation Alternatives for Ka-Band Communication Satellites," *Technical Memorandum*, NASA Glenn Research Center, 1999.

[10]. E. Matriccani and C. Riva, "Evaluation of Feasibility of Satellite Systems Design in the 10 - 100 GHz Frequency," *Inter. Journal or Satellite Commun.*, 16, pp. 237-247, 1998.

[11]. G. A. Arnold and Tai-Wu Kao, "Models Describe Rain Attenuation in EHF System." *Microwave and RF*, Penton Media, April 1996.

[12]. R. J. Acosta, "Rain Fade Compensation Alternatives for Ka-Band Communication Satellites," *Technical Memorandum*, NASA Glenn Research Center, 1999.

Appendix A

AATT Conceptual Scenarios

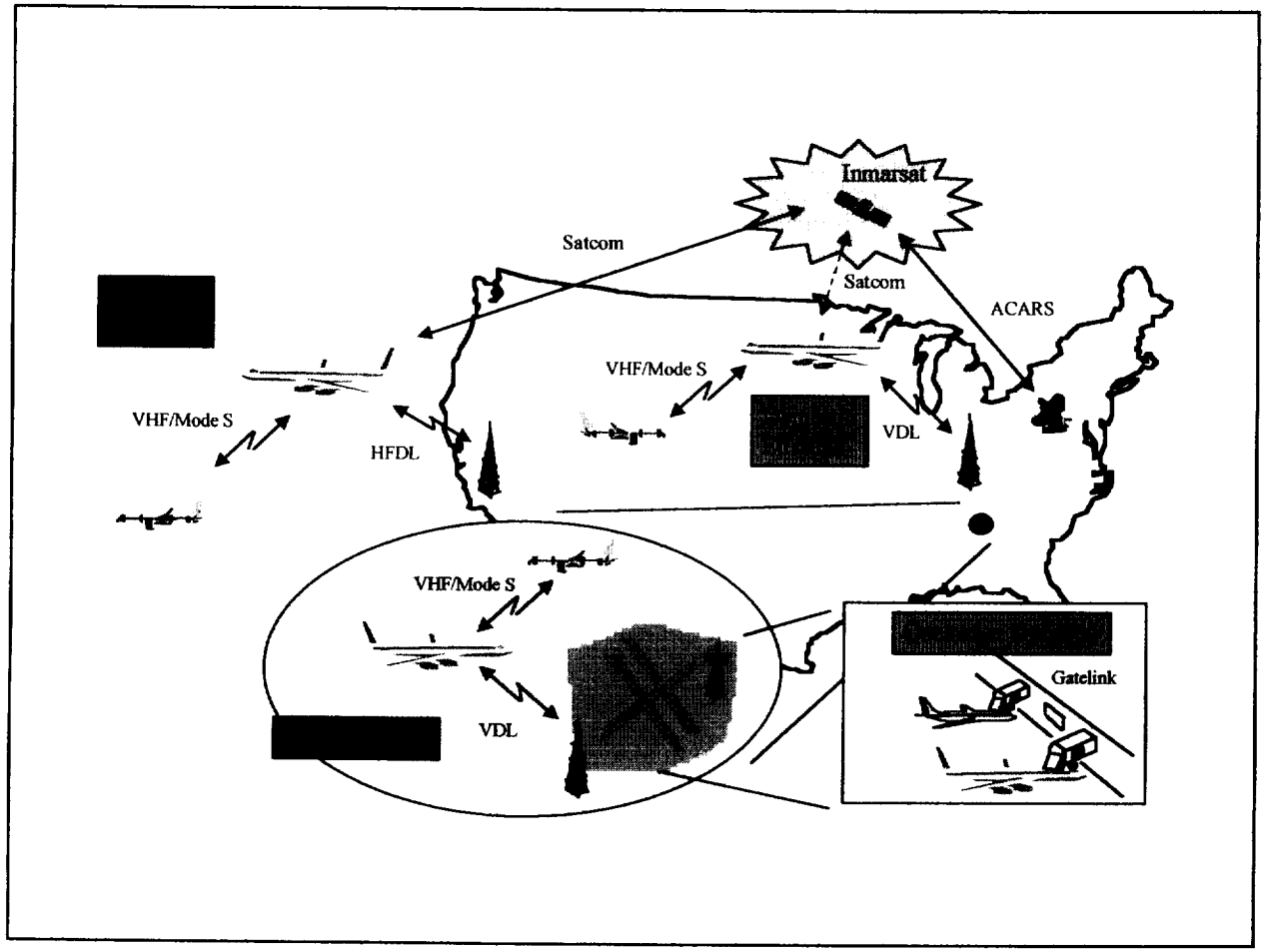

Fig. A1: Traditional Air Traffic Communication Scenarios [8]

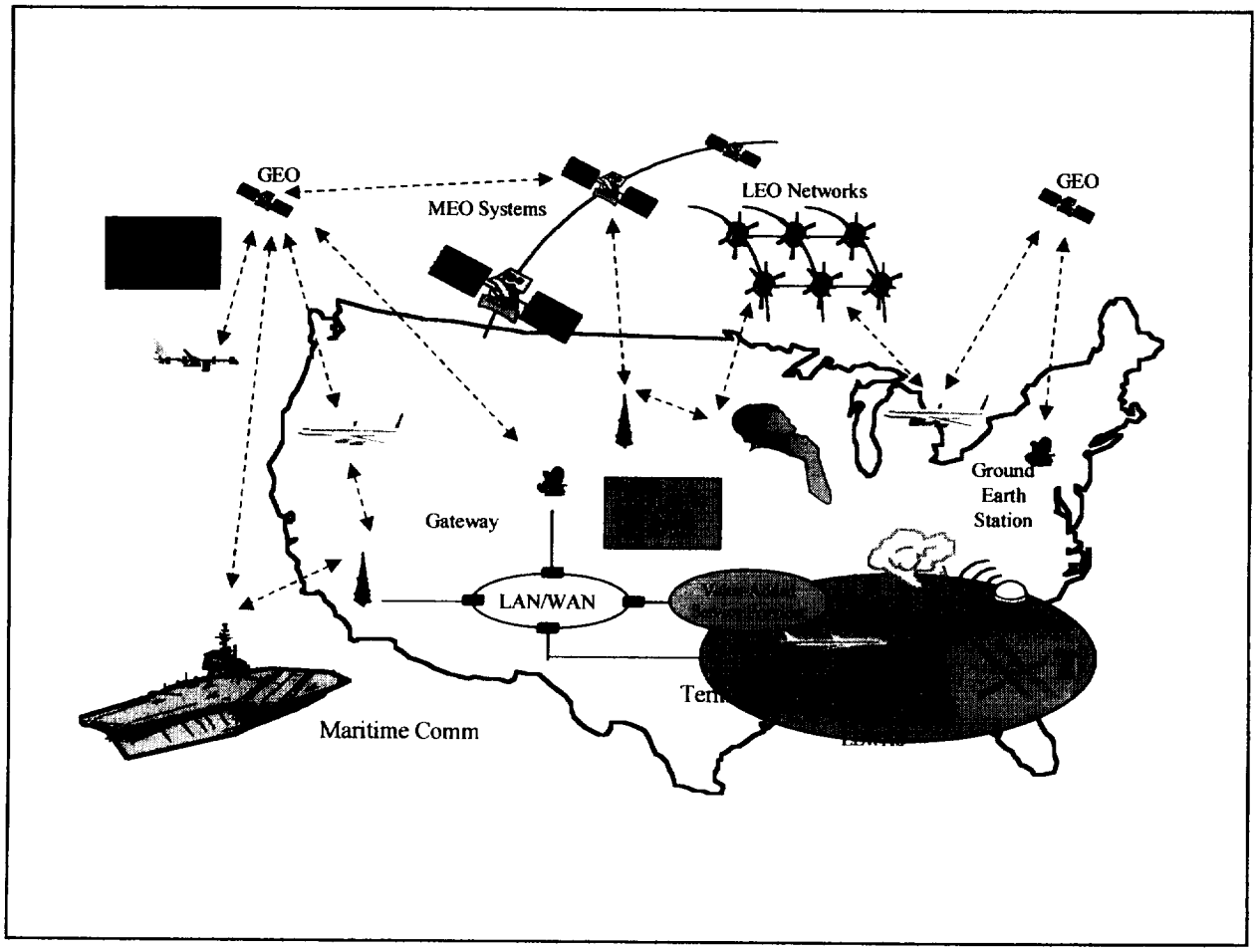

Fig. A2: Conceptual AATT Communication Scenarios

Appendix B

Identified AATT Probable Links

A. Satellite-to-Earth Station (or Control Center)

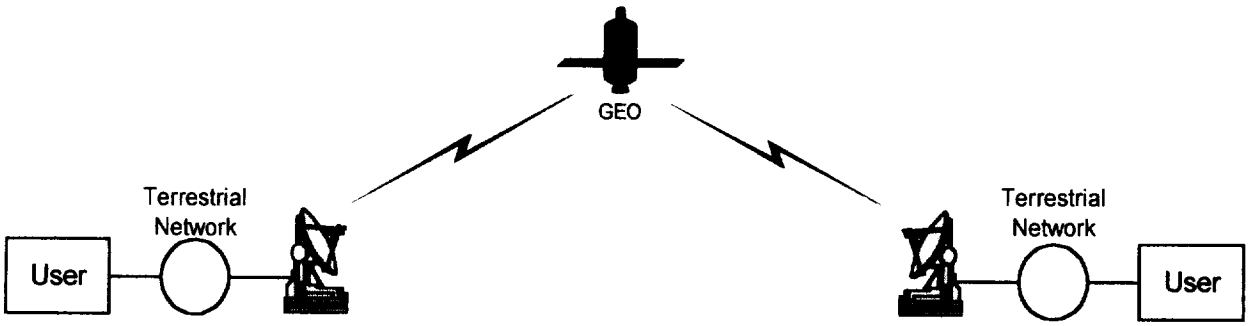

Fig. B1: Satellite-to-Earth Station (or Control Center)

B. Aircraft-to- Control Center

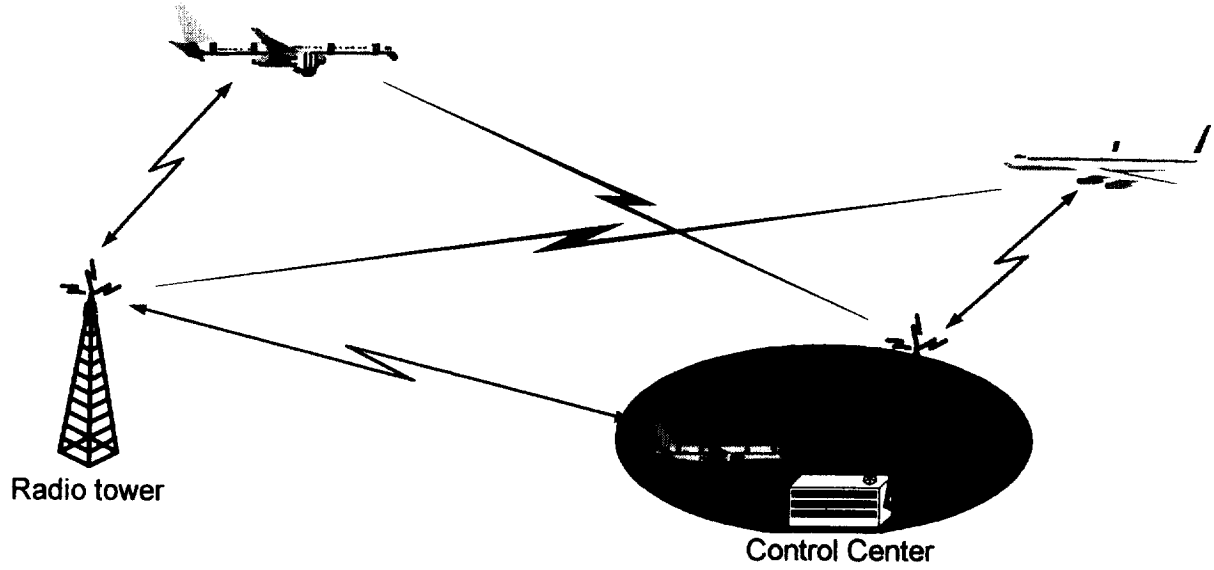

Fig. B2: Aircraft-to- Control Center

C. Aircraft-to-Aircraft

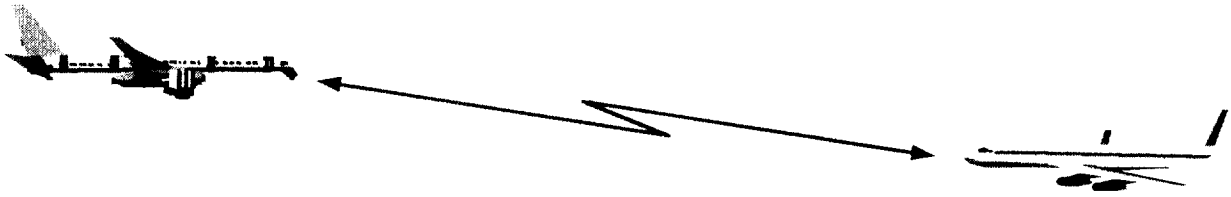

Fig. B3: Aircraft-to-Aircraft

D. Satellite-to-Aircraft

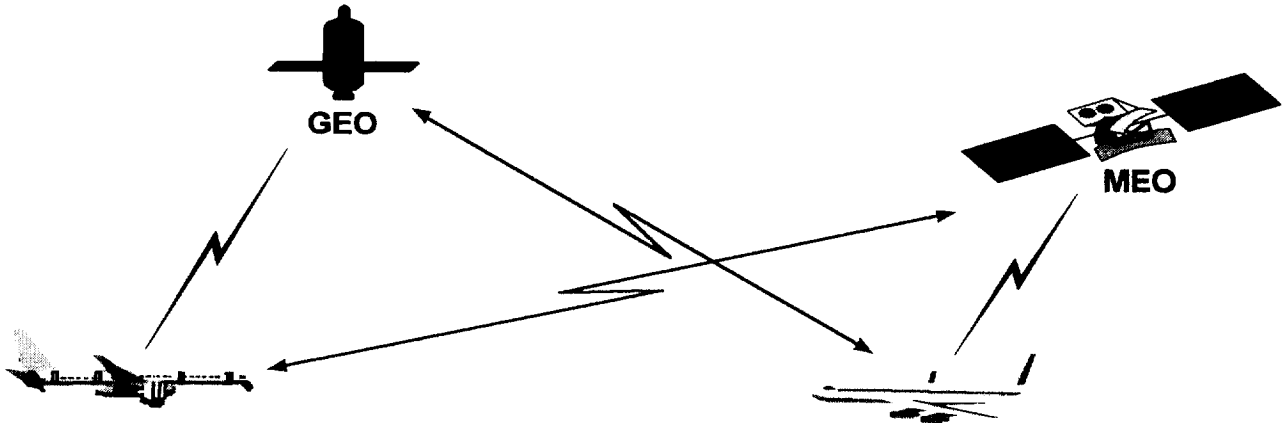

Fig. B4: Satellite-to-Aircraft

E. Satellite-to-Satellite

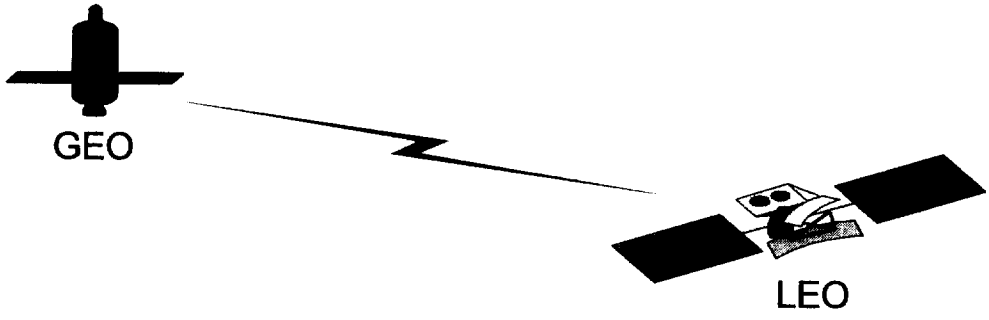

Fig. B5: Satellite-to-Satellite

Appendix C

Software Programs Contained in Floppy Diskette

The floppy diskettes attached to this report contain the simulation software developed for this project. The simulation programs are developed in MATLAB. The diskettes contain MATLAB m-files, SIMULINK model files, Graphic User Interface files, Visio diagrams and figure files. The files are correspondingly labeled. For example, files related to figure 1 in this report are correspondingly labeled FRfig1, where FR denotes Final Report.

No installation is required for the software. To run any of the supplied programs, do the following:

1. Copy all files to a directory. You make prefer to make two directories, one for the GUI programs and another for the rest of the programs
2. Start MATLAB
3. Set the location of your directory to the MATLAB path
4. At the MATLAB prompt, type any applicable *m-file* to run the m-file program
5. For the SIMULINK model, *double click* on the masked m-file in RED block.
6. For the GUI program, type *Link_Program* from the MATLAB prompt and follow the interface dialogue

We welcome any suggestions for improvement or enhancement of the routines included in this report. If you encounter any bugs or problems while operating this software, we would like to hear from you. You may contact us at the following address:

Okechukwu Ugweje, University of Akron, Akron OH 44325-3904
e-mail: ougweje@uakron.edu
URL: http://www.ecgf.uakron.edu/ugweje/web/home.html

Roberto Acosta, NASA Glenn Research Center, Cleveland OH 44135
Roberto.J.Acosta@grc.nasa.gov